Fourier Pricing of Two-Asset Options: A Comparison of Methods

Jessica Ellen Roberts

A dissertation submitted to the Faculty of Commerce, University of Cape Town, in partial fulfilment of the requirements for the degree of Master of Philosophy.

January 30, 2018

MPhil in Mathematical Finance,
University of Cape Town.

Declaration

I declare that this dissertation is my own, unaided work. It is being submitted for the Degree of Master of Philosophy in the University of the Cape Town. It has not been submitted before for any degree or examination in any other University.

January 30, 2018

Abstract

Fourier methods form an integral part in the universe of option pricing due to their speed, accuracy and diversity of use. Two types of methods in particular that are extensively used are fast Fourier transform (FFT) methods and the Fourier-cosine series expansion (COS) method.

Since its introduction the COS method has been seen to be more efficient in terms of rate of convergence than its FFT counterparts when pricing vanilla options; however limited comparison has been performed for more exotic options and under varying model assumptions. This paper will expand on this research by considering the efficiency of the two methods when applied to spread and worst-of rainbow options under two different models – namely the Black-Scholes model and the Variance-Gamma model.

In order to conduct this comparison, this paper considers each option under each model and determines the number of terms until the price estimate converges to a certain level of accuracy. Furthermore, it tests the robustness of the pricing methodologies to changes in certain discretionary parameters. It is found that although under the Black-Scholes model the COS method converges in fewer terms than the FFT method for both spread options (32 versus 128 terms) and the rainbow options (64 versus 512 terms), this is not the case under the more complex Variance Gamma model where the terms to convergence of both methods are similar. Both the methodologies are generally robust against changes in the discretionary variables; however a notable issue appears under the implementation of the FFT methodology to worst-of rainbow options where the choice of the truncated integration region becomes highly influential on the ability of the method to price accurately.

In summary, this paper finds that the improved speed of the COS method against the FFT method diminishes with a more complex model – although the extent of this can only be determined by testing for increasingly complex characteristic functions. Overall the COS method can be seen to be preferable from a practical point of view due to its higher level of robustness.

Acknowledgements

I am deeply indebted to my supervisors Peter Ouwehand and Chun-Sung Huang for their guidance and encouragement throughout. I would also like to thank Pablo Olivares and Mathew Cane for their willingness to share their expertise on the subject.

Contents

List of Figures

List of Tables

Chapter 1

Introduction

Competition between market makers has always created pressure not only to produce the "correct" price of options, but to do so quickly; with the advent of high frequency trading optimal efficiency in pricing is paramount. Furthermore, quicker and more accurate pricing is essential as every bank has to calculate the Value-at-Risk and Expected Tail Losses for all positions at the end of each day for the "end-to-end" market risk process. Numerous numerical pricing methods have been devised which can be broadly categorised into partial-(integro) differential equations (PIDE) methods, Monte Carlo simulation and Fourier-based methods. This dissertation focuses on the latter group of methods which are the most computationally efficient. In particular a comparison is presented of the Ruijter and Oosterlee's (2012) Fourier Cosine Series Expansion (COS) method and the multidimensional variant of Carr and Madan's (1999) Fast Fourier Transform (FFT) method given in Hurd and Zhou (2010) in order to answer the research question:

Is the Ruijter and Oosterlee (2012) multi-dimensional COS method more computationally efficient in calculating the price of spread and rainbow options than the Hurd and Zhou (2010) FFT method?

Thus, the crux of this dissertation amounts to determining the correct formulae for the FFT and COS-methods for a given underlying process and comparing the rate of convergence to prices and accuracy for various strike prices covering a wide range of moneyness. In order to analyse the two methods this paper makes use of both the Black Scholes model and a Variance-Gamma model – the dynamics of the latter better model the stylised facts of market returns.

This paper first introduces, in chapters 2 and 3 respectively, the necessary market models and the spread and rainbow options which serve as an underlying basis on which the analysis is implemented. Chapter 4 serves to discuss the necessary Fourier theory used in the analysis along with the original one dimensional problems for reference. Chapters 5 and 6 discuss the fast Fourier transform and COS

pricing methods, while chapter 7 presents the numerical results of the research. Finally, chapter 8 concludes.

The full tables of results have been moved to Appendix A so as not to interrupt the flow of the paper. Appendix B is used to hold other supplementary material.

Chapter 2

Asset Models

In this paper two models are employed to model stocks: the Black-Scholes (BS) model introduced originally in Black and Scholes (1973) and Madan and Seneta's (1990) Variance-Gamma (VG) model. What follows is a brief overview of the two models.

2.1 Black-Scholes Model

The Black-Scholes model serves as a benchmark against which to compare others. The appeal of the BS model is its simplicity, closed-form solutions (or accurate approximations when these are unavailable) and fair capturing of observed market data.

In the Black-Scholes model it is assumed that the risk-neutral dynamics of the underlyings are given by correlated geometric Brownian Motion (GBM). In the two-factor GBM framework the risk-neutral dynamics are given by:

$$dS_t^1 = S_t^1(r-\delta_1)dt + \sigma_1 S_t^1 dW_t^1,$$
$$dS_t^2 = S_t^2(r-\delta_2)dt + \sigma_2 S_t^2 dW_t^2,$$

where (S_t^1, S_t^2) are the prices of the underlying at time t, r is the risk-free rate, (W_t^1, W_t^2) are risk-neutral Wiener processes with constant correlation ρ, the corresponding volatilities $\sigma = (\sigma_1, \sigma_2)$ and the dividend yields $\delta = (\delta_1, \delta_2)$.

The joint characteristic function of $X_T = (\ln(S_T^1), \ln(S_T^2))$, where T is the maturity of the option, as a function of $u = (u_1, u_2)$ is of the form $e^{iuX_0'}\phi(u;T)$ with

$$\phi(u;T) = \exp\left[iuT\left(r\mathbf{1} - \frac{\sigma^2}{2}\right)' - \frac{u\Sigma u'T}{2}\right] \tag{2.1}$$

where $\mathbf{1} = (1,1), \Sigma = \begin{bmatrix} \sigma_1^2 & \sigma_1\sigma_2\rho \\ \sigma_1\sigma_2\rho & \sigma_2^2 \end{bmatrix}$ and $\sigma^2 = diag(\Sigma)$.

Finally – as will be discussed in chapter 6 – for the implementation of the COS-method one needs the first, second and fourth cumulants of the process underlying the market model in order to determine the truncated domain of integration. The cumulants of a random variable are defined via the cumulant-generating function – the natural logarithm of the moment generating function.

Definition 2.1 (Cumulants)**.** Given a real random variable whose moment generating function is given as $M(u) = \mathbb{E}[e^{uX}]$ and taking the logarithm of this function, expressing it as its power series gives the cumulant generating function as:

$$K(u) := (\log[M])(u) = \sum_{n=0}^{\infty} \frac{\kappa_n u^n}{n!}.$$

The coefficients of the expansion $\kappa_1, \kappa_2, \ldots$ are the cumulants of the random variable. One can note that $\kappa_n = K^{(u)}(0)$ for all n.

These expressions can either be derived from first principles or readily found in table 5.2 of Kienitz and Wetterau (2012) which gives the cumulants necessary for many of the popular stock models, and in particular the GBM and VG models.

Tab. 2.1: Cumulants of the GBM process required for COS-method

Cumulants of the GBM Process	
c_1	$T(r - \delta - \frac{\sigma^2}{2})$
c_2	$T\sigma^2$
c_4	0

2.2 Lévy Models

Exponential Lévy models serve to generalise the classical Black-Scholes model discussed above in Section 2.1 by maintaining the stationarity and independence of increments but introducing the presence of jumps. There are various reasons for introducing jumps which are discussed in depth in Tankov (2011). In brief the most important of these are as follows:

- Markets simply do jump for a multitude of reasons (dividends paid, news coverage, micro-crashes etc.).
- The introduction of jumps can explain the volatility smile observed in markets. Although this smile can also be emulated using a continuous stochastic

or local volatility model, the fact that the smile tends to become more prominent as the time horizon shortens points to the existence of jumps as the culprit (flattening as time horizon lengthens occurs as a result of the "large deviation" theory – for more discussion of this the reader can refer to Bucklew (2004) or Touchette (2009)) .

- Jump processes correspond to incomplete markets which is congruent with our reality (since completeness of markets is mostly a theoretical concept) whereas continuous models are either complete or "completable". This incompleteness makes rigorous analysis of hedging errors possible, which is critical for the improvement of these errors.

Lévy models have the above modelling advantages, whilst still remaining mathematically tractable as their characteristic functions are always known (Barndorff-Nielsen *et al.*, 2012) and can be obtained via the Lévy-Khintchine representation presented in section 2.2.1.

Most likely as a result of all of the above advantages, there exists a plethora of Lévy models used in mathematical finance alone. A few of the important definitions and results relating to Lévy processes – and thus models – are discussed below in section 2.2.1.

2.2.1 Important Definitions and Results for Lévy Processes

This section serves to briefly define and discuss a handful of the most important facts needed in the implementation of Lévy models in Fourier pricing methods. All of the following material can be found in various works such as Tankov (2003), Schoutens (2003) and Barndorff-Nielsen *et al.* (2012) which can be referred to for a more in-depth discussion of Lévy processes and their history.

Lévy Processes

Lévy models are defined by their underlying Lévy process, where a Lévy process is defined as follows.

Definition 2.2 (Lévy Process)**.** A Lévy process is a real-valued and adapted process $X = (X_t)_{0 \leq t < \infty}$ which satisfies the following conditions:

i) $X_0 = 0$ a.s.;

ii) it has independent increments (i.e. for any $0 \leq t_0 < t_1 < \cdots < \infty$ it holds that increments $X_0, X_{t_1} - X_{t_0}, \ldots X_{t_n} - X_{t_{n-1}}$ are independent);

iii) it has stationery, or time-homogeneous, increments (i.e for any $s < t$, $X_t - X_s$ has the same distribution as X_{t-s});

iv) it is stochastically continuous (i.e. for all $\epsilon > 0$ and $s, t > 0$ it holds that $\mathbb{P}(|X_{t+s} - X_s| > \epsilon) \to 0$ as $t \to 0$);

v) as a function of t the process is càdlàg (i.e. is right-continuous with left limits).

One can note that the Wiener process (or Brownian Motion if one prefers) is thus by Definition 2.2 a Lévy process, and therefore the results from here also hold for the processes in section 2.1.

All processes that satisfy the first three properties are known as *processes with independent stationary increments (PIIS)*. An important property of the PIIS class is that the distribution of any member of this class is determined completely by the law of X_1.

Furthermore, it can be noted that properties (ii) and (iii) of definition 2.2 – i.e. the fact that the increments of a Lévy process are independent and stationary – imply that Lévy processes are by definition Markov processes. In fact they are Strong Markov processes as they are càdlàg.

Infinitely Divisible Processes

Definition 2.3 (Infinitely Divisible Distribution)**.** Let X be a real-valued random variable with law μ_X. X is said to be infinitely divisible if:

i) for every $n \in \mathbb{N}$ there exists independent identically distributed (i.i.d.) random variables $Y_0^{(n)}, \dots Y_n^{(n)}$ such that

$$X \stackrel{d}{=} Y_1^{(n)} + \ldots + Y_n^{(n)},$$

or equivalently

ii) there exists a probability measure $\mu_Y^{(n)}$ such that $\mu_X = \mu_Y^{(n)} * \ldots * \mu_Y^{(n)} := (\mu_Y^{(n)})^{n*}$ which denotes the n-fold convolution of $\mu_Y^{(n)}$.

There exists a bijection between a Lévy process and the class of infinitely divisible distributions: if X is a Lévy process then $X_t = X_{t/n} + (X_{2t/n} - X_{t/n}) + \cdots + (X_{(n-1)t/n} - X_t)$ is a sum of i.i.d. random variables and so X_t is infinitely divisible; conversely, it can be shown that if μ is infinitely divisible, there is a Lévy process X such that X_1 has distribution μ. Thus one can speak of either a particular Lévy process or the related infinitely divisible distribution. This fact allows us to use the Lévy-Khintchine representation (which holds for all infinitely divisible distributions) in order to determine the characteristic function of a Lévy process.

Lévy-Khintchine Representation

In general, the distribution of a Lévy process is determined by its characteristic function which is given by the Lévy-Khintchine formula from the following theorem.

Theorem 2.4 (Lévy Khintchine Representation of the Lévy Characteristic Function)**.** *If X_t is a Lévy process, then it has a characteristic function $\phi_X(u,t)$ given by:*

$$\phi_X(u,t) = e^{t\Psi(u)}$$

where the characteristic exponent ,$\Psi(u)$, is given by:

$$\Psi(u) = \gamma\theta i - \frac{1}{2}\sigma^2 u^2 + \int_{\mathbb{R}\setminus\{0\}} \left(e^{iux} - 1 - iux\mathbb{1}_{|x|<1}\right)\Pi(dx)$$

where $\gamma \in \mathbb{R}, \sigma \geq 0$ and Π is known as the Lévy measure (which is unique) and satisfies

$$\int_{\mathbb{R}\setminus\{0\}} (x^2 \wedge 1)\Pi(dx) < \infty$$

Thus since the distribution of a random variable is uniquely determined by its characteristic function, this means that a Lévy process can be represented by the triplet (γ, σ, Π) which is known as the Lévy-Khintchine triplet where γ is the drift, σ^2 the variance and $\Pi(x)$ the "jump measure" which gives the arrival rate of jumps of size x.

2.2.2 Variance-Gamma Model

The Variance-Gamma (VG) model was first introduced by Madan and Seneta (1990) who presented a symmetric version of the model which allowed for an adjustment of kurtosis but not skewness. The model was later extended by Madan *et al.* (1998) allowing for an asymmetric form of the VG process – thus allowing for skewness – and further presenting formulae to allow for pricing vanilla European options with underlyings that follow VG model dynamics.

The intention when introducing the VG model was to create a model which was both practical and able to provide more reasonable dynamics than the classic GBM described above in section 2.1 through its ability to cater for a wider modelling of skewness and kurtosis (Kienitz and Wetterau, 2012) – which according to various empirical investigations (Dushimimana, 2010; Figueroa-López *et al.*, 2011; Göncü *et al.*, 2013) it is able to do about as well as more complex Lévy models such as the CGMY model.

There are two ways in which one can express the Variance-Gamma process, either as the difference of two Gamma processes or as a Brownian Motion, $X(t) :=$

$W(Y(t))$, time-changed by an independent Gamma process $Y(t)$. The latter methodology specifically views the VG process as an extension of Brownian Motion obtained by evaluating a normal process at random time points which are defined by an independent Gamma process, i.e. the time variable of a Brownian Motion becomes a stochastic variable given by a Gamma process (Fiorani, 2004).

More specifically a d-dimensional VG process can be stated as:

$$X_t^i = \theta_i Y_t + \sigma_i W_{Y_t}^i, i = 1, ..., d$$

where $W^i = (W_t^i); t \geq 0)$ is a d-dimensional standard Brownian Motion with drift θ_i and volatility σ_i, and Y_t the Gamma process with unit mean and a variance of ν.

The Gamma process Y_t is known as a *subordinator*: a one dimensional Lévy process which is non-decreasing almost surely – which is consistent for the definition of a time variable. One can interpret each unit of calender time as having an "economically relevant" time length associated with it – the "economic time unit" given by this Gamma process (Madan *et al.*, 1998). So although the number of economic time units in the corresponding calendar unit is expected on average to be one, this may differ depending on the situation in the economy. This is reflected in the Gamma process which is therefore given a mean of one and a variance depicting the uncertainty associate with the economic time unit's length.

Following a version of Leoni and Schoutens (2008) approach, the risk-neutral dynamics of the underlyings in the two-dimensional VG framework are:

$$\begin{aligned} dS_t^1 &= S_t^1 \left[(\mu_1 dt + \theta_1 Y_t) + \sigma_1 dW_{Y_t}^1 \right] \\ dS_t^2 &= S_t^2 \left[(\mu_2 dt + \theta_2 Y_t) + \sigma_2 dW_{Y_t}^2 \right] \end{aligned}$$

where $\mu_i = (r - \delta_i) + \frac{1}{\nu} \ln\left(1 - \frac{1}{2}\nu\sigma_i^2 - \theta_i \nu\right)$ for $i = 1, 2$.

The joint characteristic function of $X_T = (\ln(S_T^1), \ln(S_T^2))$, as a function of $u = (u_1, u_2)$ is of the form $e^{iuX_0'}\phi(u; T)$ with

$$\phi(u; T) = [\phi(u, 1)]^T = \exp(i\mu u') \left(\mathbf{1} - i\nu u\theta' + \frac{1}{2}\nu u \Sigma u' \right)^{-T/\nu} \tag{2.2}$$

where $\mu = (\mu_1, \mu_2), \theta = (\theta_1, \theta_2)$ and $\mathbf{1}, \Sigma$ are defined as with the Black Scholes model in section 2.1.

Finally, for the implementation of the COS-method, the necessary cumulants are shown in Table 2.2:

Tab. 2.2: Cumulants of the VG process required for COS-method

Cumulants of the VG Process	
c_1	$T(r-\delta+\theta)$
c_2	$T(\sigma^2+\nu\theta^2)$
c_4	$3T(\sigma^4\nu+2\theta^4\nu^3+4\sigma^2\theta^2\nu^2)$

Chapter 3

Spread and Rainbow Options

Both the spread and rainbow options considered in this paper are European in nature and involve two underlying assets. Spread options are widely used within industry (Carmona and Durrleman, 2003) whereas rainbow options are less so, but still relevant particularly in the area of "real options" (Copeland and Keenan, 1998).

The pricing of all two-dimensional options (and thus the pricing of spreads and two-coloured rainbow options) comes down to the calculation of the following formula for the value of the option currently, $v(t_0, \mathbf{x})$, based off the payoff of the option at maturity given by $v(T, \mathbf{y})$:

$$v(t_0, \mathbf{x}) = e^{-r\Delta t}\mathbb{E}_{\mathbb{Q}}^{t_0,\mathbf{x}}\left[v(T, \mathbf{y})\right] = e^{-r\Delta t}\int\int_{\mathbb{R}^2} v(T, \mathbf{y}) f(\mathbf{y}|\mathbf{x}) d\mathbf{y} \tag{3.1}$$

where $\mathbf{x}$ is the current log-asset value vector, $\mathbf{y}$ is the log-asset value vector at time T, $f(\mathbf{y}|\mathbf{x})$ is the conditional density function of the final log-asset prices ($\mathbf{y}$) given the current log-asset price ($\mathbf{x}$) at time t_0. r is the risk-free rate and $\Delta t := T - t_0$ is the time to maturity and the expectation refers to the conditional expectation under the risk-neutral measure.

3.1 Payoff and Pricing Equation

In both cases call options are considered, but similar analysis can be done for put options or alternatively put option prices can be obtained through put-call parity relationships.

3.1.1 Spread Call

In this paper we consider a long European spread call on two assets S_t^1 and S_t^2 with a strike of K, maturity T and fixed weighting parameters a and b which gives a payoff at time T of:

$$C_T = \left(aS_T^1 - bS_T^2 - K\right)^+ \tag{3.2}$$

where $(x)^+ := \max\{x, 0\}$

The weighting parameters are used for cases where one is writing a spread option on assets with vastly different values so that S^1 and S^2 are more comparable. For the purpose simplicity in this dissertation it is taken that $a = b = 1$ and so the above equation simplifies to the following:

$$C_T = \left(S_T^1 - S_T^2 - K\right)^+. \tag{3.3}$$

Thus, using usual risk-neutral pricing we have that the value of the option at time t_0 is given by the expression:

$$C_{t_0} = e^{-r\Delta t}\mathbb{E}_{\mathbb{Q}}\left[\left(S_T^1 - S_T^2 - K\right)^+\right] \tag{3.4}$$

where r is the risk-free rate of interest and the expectation is taken with respect to the equivalent martingale measure (EMM).

3.1.2 Rainbow On-The-Min Payoff

Similarly, we consider a long European call on-the-min of two assets which gives a payoff of:

$$C_T = \left(\min\left(S_T^1, S_T^2\right) - K\right)^+. \tag{3.5}$$

Which in turn gives a similar expression for the price of the option at time t_0:

$$C_{t_0} = e^{-r\Delta t}\mathbb{E}_{\mathbb{Q}}\left[\left(\min\left(S_T^1, S_T^2\right) - K\right)^+\right]. \tag{3.6}$$

Analysis can also be done for options on-the-max following similar processes implemented in this dissertation, or by the use of "min-max parity" relationship (as dubbed in Ouwehand and West (2006)) stated in Stulz (1982):

$$C_{max}(S_T^1, S_T^2, K, T) = C(S_T^1, K, T) + C(S_T^2, K, T) - C_{min}(S_T^1, S_T^2, K, T)$$

where $C_{max}(S_T^1, S_T^2, K, T)$ is the price of a rainbow call on-the-max of two assets S^1 and S^2, with strike K and time to maturity T. $C_{min}(S_T^1, S_T^2, K, T)$ is the call on-the-min and $C(S_T^i, K, T)$ the vanilla call for each asset.

3.2 Industry Use

3.2.1 Spread Options

Spread options are pervasive within financial markets as a whole (this popularity can be attributed to their ability to mitigate against adverse movements of several

indexes) and liquid in developed equity, foreign exchange, fixed income and commodities markets. This extreme diversity of underlyings can be considered to be part of the cause of the wide variety of models and pricing methodologies appearing in the literature. For further reference Carmona and Durrleman (2003) which provides an excellent summary of the methodologies used and difficulty associated with the pricing of spread options.

Some of the most common uses and types of spread options are explained below.

Currency Spreads

When the underlying assets to a spread option are different exchange rates, the option is then known as a currency spread option. These instruments can be used for both speculative and hedging objectives, and often involve the currencies of countries with closely related economies.

Fixed Income Spreads

These spread options involve the difference between multiple interest or swap rates. The most liquid options in developed financial markets are options on spreads between rates of different maturities (which can give an indication of default risk) as well as spreads between quality levels of lenders.

Commodity Future Spreads

Commodity spread options seem to make up the majority of spread option contracts, likely due to their hedging abilities. Two broad categories of commodity spread options are *single commodity spread options* and *cross-commodity spread options*.

Single commodity options are less pervasive and most can be categorised as location spread options (options on the spread between the same commodity at different locations which can act as a hedge against transmission or transportation risk exposure) or temporal/calendar spread options – which are options on the same commodity but at two different dates in the future.

Cross-commodity spread options include quality spread options (options on the difference between different grades of the same commodity) and processing spread options (options based on the difference between the prices of inputs and outputs of a production process). Processing spread options are important hedging instrument as the spread can be seen as a way to quantify the cost of production of a refined good from the raw materials used to make it.

Specific and important examples of processing spreads can be found in the agricultural and energy markets. Crush spreads options are based on the difference between the meal and oil extracted from a bushel of soy-beans and the prices of a bushel of soy-beans. These are important options in the agricultural futures market – so much so that they are in fact exchange-traded over the Chicago Board of Trade. The energy market has two main types of spread options: spark spread options (the primary cross-currency transaction in the electricity market) and crack spread options. Spark spreads are defined as the difference between the price of electricity developed by a generator and the cost of the fuel used in order to generate that electricity. Crack spreads on the other hand are the simultaneous purchase/sale of crude oil and sale/purchase of a refined petroleum product.

As one can see from the above discussion spread options are a fairly important part of the financial markets and although they are still predominantly traded over-the-counter (OTC), they are making their way into exchanges which motivates the need for a faster pricing methodology than the next market-maker.

3.2.2 Rainbow Options

Rainbow options on-the-max and on-the-min (also called best-of and worst-of rainbow options respectively) are not as liquidly traded as spreads and almost always traded OTC. As a result, the speed at which one obtains a price is not as important for the moment; however this might change in the future as there are various industry uses for rainbow options.

Most notably, rainbow options allow for greater exposure to the market at a cheaper cost than through portfolio diversification and hedging (Klyueva, 2014), while still allowing for the benefits of reduced risk exposure and expanded investment opportunities. This makes rainbow options useful for various portfolio managers.

Best-of options could also be used for hedging purposes. An example of such would be a currency hedge whereby a company with the option of settling their expenses in various foreign currencies at some point in the future could purchase a best-of call (Guillaume, 2008).

Finally, worst-of calls are often made use of in so-called "real option" valuation where the embedded options of projects created by certain agreements gives rise to the use of these methods to value things other than financial options. for example "fuel switching" allows an operation to choose either gas or coal as fuel, which could be valued as a worst-of option as the cheapest fuel should be chosen (Detemple *et al.*, 2003).

3.3 Benchmarks

For a "sanity check" on the prices produced as well as a means to determine the accuracy of the methods this paper makes use of the existing closed-form approximations when modelling under geometric Brownian Motion and Monte Carlo (MC) pricing methodology when making use of the Variance-Gamma model using the method explained in Kienitz and Wetterau (2012) to simulate the Variance-Gamma process.

3.3.1 Approximations Under Geometric Brownian Motion

For the spread options the Bjerksund and Stensland (2014) valuation formula is used as it is shown to be highly accurate, more so than the Kirk (1995) approximation – particularly when the option is far-in or -out the money – which was previously used in the literature for comparison. For a full description of this valuation technique one can refer to the original paper.

For best-of valuations only one closed form valuation expression is known, namely the Stulz price. It too has been shown to be highly accurate and used in the literature as a benchmark for pricing methods. For a more detailed explanation of this method the reader can refer to Stulz (1982).

Chapter 4

Fourier Theory and One-Dimensional Fourier Finance

4.1 Fourier Transform Pair

Definition 4.1 (Direct Fourier Transform)**.** The Fourier transform of a (one-dimensional) real-valued function $g(t), t \in \mathbb{R}$ can be defined by

$$\mathcal{F}\{g(t)\}(u) := \int_{-\infty}^{\infty} e^{iut} g(t) dt. \tag{4.1}$$

For ease of notation we define $\hat{g}(u) := \mathcal{F}\{g(t)\}(u)$.

Definition 4.2 (Inverse Fourier Transform)**.** The corresponding inverse Fourier transform can then be defined

$$\mathcal{F}^{-1}\{\hat{g}(u)\}(t) := \frac{1}{2\pi} \int_{-\infty}^{\infty} e^{-iut} \hat{g}(u) du. \tag{4.2}$$

$g(t)$ and $\hat{g}(u)$ are what is known as the Fourier transform pair and it holds that $g(t) = \mathcal{F}^{-1}\{\hat{g}(u)\}(t)$.

Definition 4.3 (Multi-Dimensional Fourier Transform)**.** The above definitions in equations 4.1 and 4.2 hold in the multivariate case where $\mathbf{t}$ and $\mathbf{u}$ are vectors of length n:

$$\hat{g}(\mathbf{t}) := \int \cdots \int_{\mathbb{R}^n} e^{i\mathbf{u}\cdot\mathbf{t}} g(\mathbf{t}) d\mathbf{t}, \tag{4.3}$$

$$g(\mathbf{u}) := \left(\frac{1}{2\pi}\right)^n \int \cdots \int_{\mathbb{R}^n} e^{-i\mathbf{u}\cdot\mathbf{t}} \hat{g}(\mathbf{u}) d\mathbf{u}. \tag{4.4}$$

4.1.1 Link to Characteristic Functions

Definition 4.4 (Characteristic Function)**.** A random variable $\mathbf{X} = (X_1, ..., X_n)$ with joint probability density function $f_{\mathbf{X}}(x_1, ..., x_n)$ has a characteristic function defined

by

$$\begin{aligned}\phi_{\mathbf{X}}(u_1, ..., u_n) &:= \mathbb{E}\left[e^{i(u_1x_1+...+u_nx_n)}\right] \\ &= \int \cdots \int_{\mathbb{R}^n} e^{i\mathbf{u}\cdot\mathbf{X}} f_{\mathbf{X}}(x_1, ...x_n)dx_1...dx_n.\end{aligned}$$

From definition 4.4 and equation 4.1 we can see that the characteristic function of a random variable is equivalent to the Fourier transform of the variable's probability function. In other words it holds that:

$$\mathcal{F}\{f_{\mathbf{X}}\}(\mathbf{u}) \equiv \phi_{\mathbf{X}}(\mathbf{u}). \tag{4.5}$$

The relation defined in equation 4.5 allows one to make use of the Fourier transform in pricing options, since if one has the characteristic function of the distribution of the underlying we are able to reconstruct the density function using the inverse transform and thus use risk-neutral pricing formula given by equation 3.1. Uniqueness of the distribution is ensured by the Lévy Inversion Theorem (Chung, 2001):

Theorem 4.5 (Lévy's Inversion Theorem)**.** *Two random variables (say X and Y) have the same characteristic functions (ϕ_X and ϕ_Y) if and only if they have the same distribution.*

4.1.2 Discrete Fourier Transform

In order to perform the numerical integration computations needed in Fourier methods, one needs a discrete version of the Fourier transform. The standard formulation of the (one dimensional) discrete Fourier transform (DFT) is given as follows:

Definition 4.6 (Discrete Fourier Transform)**.** Let $x_0, x_1, ..., x_{N-1}$ be a sequence of N complex numbers. The DFT of this sequence is defined by:

$$DFT(x_m) = \hat{x}_m = \sum_{n=0}^{N-1} e^{-i\frac{2\pi}{N}nm} x_n.$$

Similarly, the Inverse DFT (IDFT) is given then as

$$x_n = \frac{1}{N}\sum_{m=0}^{N-1} e^{i\frac{2\pi}{N}nm}\hat{x}_m.$$

One can view the DFT as a (scaled) discrete approximation of the inverse Fourier transform and the IDFT as one for the direct Fourier transform. As with the continuous case there exist multi-dimensional forms of the direct and inverse DFT, in this paper we make use of the 2D version:

Definition 4.7 (2-Dimensional Discrete Fourier Transform)**.**

$$DFT(x_{u,v}) = \hat{x}_{u,v} = \sum_{n=0}^{N-1}\sum_{m=0}^{M-1} x_{n,m} e^{-i2\pi\left(\frac{un}{N}+\frac{vm}{M}\right)} \tag{4.6}$$

$$IDFT(x_{n,m}) = x_{n,m} = \frac{1}{NM}\sum_{u=0}^{N-1}\sum_{v=0}^{M-1} \hat{x}_{u,v} e^{i2\pi\left(\frac{un}{N}+\frac{vm}{M}\right)} \tag{4.7}$$

4.2 Fourier-Cosine Transform

There exists both Fourier-sine and -cosine series expansions. The Fourier-sine series expansion has been used in option pricing namely in Meng and Ding (2013); however this is an exception and usually Fourier-cosine derived methods are used – in particular those in Fang and Oosterlee (2008) and Ruijter and Oosterlee (2012). Thus only the Fourier-cosine transform is considered in this paper.

Similar to the Fourier-transform discussed in Section 4.1, the continuous version of the Fourier-cosine expansion is of little use in numerical applications and is thus defined below for its use in the derivation of the COS-method formula rather than its practical use.

Definition 4.8 (Fourier-Cosine Series Expansion)**.** Given an integrable function $f(x)$ with support $[a,b] \in \mathbb{R}$ the Fourier-cosine expansion of $f(x)$ is given by:

$$f(x) = \sum_{n=0}^{\infty}{}' A_n \cos\left(n\pi\frac{x-a}{b-a}\right)$$

where $\sum'$ indicates that the first term (where $n=0$) in the summation is weighted by a half and

$$A_n = \frac{2}{b-a}\int_a^b f(x)\cos\left(n\pi\frac{x-a}{b-a}\right)dx.$$

Which again has a multi-dimensional version for a vector $\mathbf{x}$ of length m and $f(\mathbf{x})$ with support $[a_1,b_2]\times ...\times [a_m,b_m]\in\mathbb{R}^m$:

$$f(\mathbf{x}) = \sum_{n_1=0}^{\infty}{}' \cdots \sum_{n_m=0}^{\infty}{}' A_{n_1,\ldots,n_m}(\mathbf{x}) \cos\left(n_1\pi\frac{x_1-a_1}{b_1-a_1}\right)\ldots\cos\left(n_m\pi\frac{x_m-a_m}{b_m-a_m}\right) \tag{4.8}$$

where $\{A_{k_1,k_2}(\mathbf{x})\}_{k_1,k_2}$ are the cosine series coefficients which are defined:

$$A_{n_1,\ldots,n_m} := \frac{2}{b_1-a_1}\cdots\frac{2}{b_m-a_m}\int_{a_1}^{b_1}\cdots\int_{a_m}^{b_m} f(\mathbf{x})\cos\left(n_1\pi\frac{x_1-a_1}{b_1-a_1}\right)\ldots \cos\left(n_m\pi\frac{x_m-a_m}{b_m-a_m}\right)d\mathbf{x}. \tag{4.9}$$

4.2.1 Discrete Fourier-Cosine Transform

The variant of the discrete cosine transform (DCT) used in this paper is type-II DCT, which will simply be referred to as "the DCT", and the inverse of this – a scaled type-III DCT – will be referred to as "the inverse DCT".

Definition 4.9 (The Type-II Discrete Fourier Transform)**.** Let $x_0, x_1, ..., x_{N-1}$ be a sequence of N real numbers. The DCT of this sequence is defined by:

$$DCT(x_m) = \sum_{n=0}^{N-1} x_n \cos\left[\frac{\pi}{N}\left(n+\frac{1}{2}\right)m\right].$$

Similarly, the inverse DCT is defined by:

$$\begin{aligned} IDCT(x_n) &= \frac{2}{N}\left[\frac{1}{2}x_0 + \sum_{m=1}^{M-1} x_m \cos\left[\frac{\pi}{M}\left(m+\frac{1}{2}\right)n\right]\right] \\ &= \frac{2}{N}\sum_{n=0}^{N-1}{}' x_m \cos\left[\frac{\pi}{M}\left(m+\frac{1}{2}\right)n\right]. \end{aligned}$$

Again, a multidimensional version exist and of particular use in this paper is the 2D transform and inverse:

$$DFT(x_{u,v}) = \sum_{n=0}^{N-1}\sum_{m=0}^{M-1} x_{n,m} \cos\left[\frac{\pi}{N}\left(n+\frac{1}{2}\right)u\right] \cos\left[\frac{\pi}{M}\left(m+\frac{1}{2}\right)v\right] \tag{4.10}$$

$$IDCT(x_{n,m}) = \frac{2}{N}\frac{2}{M}\sum_{u=0}^{N-1}{}'\sum_{v=0}^{M-1}{}' x_{u,v} \cos\left[\frac{\pi}{N}\left(u+\frac{1}{2}\right)n\right] \cos\left[\frac{\pi}{M}\left(v+\frac{1}{2}\right)n\right] \tag{4.11}$$

4.3 One-Dimensional Fourier Pricing

The following section discusses the outline of the evolution of Fourier (or characteristic function based) pricing methodologies in finance, with particular reference to Carr and Madan (1999) and Fang and Oosterlee (2008).

Some of the earlier works on the topic used the fact that if the characteristic function of the underlying process is known analytically, a way to determine the value of a vanilla call on an underlying with current price S_{t_0}, with strike K, and expiring after a period of T would be to use the Gil-Pelaez (1951) formula:

$$C = S_{t_0}\Pi_1 - Ke^{-rT}\Pi_2 \tag{4.12}$$

where r is the (constant) risk-free rate and Π_1 is the delta of the option given by

$$\Pi_1 = \frac{1}{2} + \frac{1}{\pi}\int_0^\infty \text{Re}\left[\frac{e^{-iu\ln(K)}\phi_T(u-i)}{iu\phi_T(-i)}\right]du,$$

and Π_2 is the risk-neutral probability of finishing in-the-money:

$$\Pi_2 = \frac{1}{2} + \frac{1}{\pi}\int_0^\infty \text{Re}\left[\frac{e^{-iu\ln(K)}\phi_T(u)}{iu}\right] du,$$

where $\phi_T(u)$ is the characteristic function of the log-price of the asset under the T-forward measure $\mathbb{Q}^T$.

The integrals in Π_1 and Π_2 are determined numerically; however the fast Fourier transform (FFT) methods cannot be used to speed up this process due to the singularity at $u = 0$. This inspired the work of Carr and Madan (1999).

4.3.1 Carr and Madan (1999) Fast Fourier Transform Pricing

Again we consider C the current price of a vanilla call on an underlying S_t, with strike K, and time to expiry of T. Letting $f_T(x)$ and $\phi_T(u)$ be the density and characteristic function of $\ln(S_T)$ under the the risk-neutral measure $\mathbb{Q}$ and r be the risk-free rate. Furthermore, define $s_T = \ln(S_T)$ and $k = \ln(k)$ which gives:

$$\begin{aligned} C &= e^{rT}\mathbb{E}_\mathbb{Q}\left[(S_T - K)^+\right] \\ &= e^{rT}\int_k^\infty (e^s - e^k) f_T(s) ds \end{aligned}$$

which is not L^1-integrable with respect to the log-strike price. In order to obtain a square integrable function Carr and Madan (1999) consider a dampened or modified call price defined by:

$$c_T(k) := e^{\alpha k} C_T(k)$$

where $\alpha > 0$ and thus gives its Fourier transform as:

$$\begin{aligned} \psi_T(\theta) &:= \int_{-\infty}^\infty e^{i\theta k} c_T(k) dk \\ &= e^{rT}\frac{\phi_T\left(\theta - i(\alpha+1)\right)}{(i\theta+\alpha)(i\theta+\alpha+1)} \end{aligned}$$

which allows them to solve for C_T in terms of $\psi_T(\theta)$ – if $c_T(k) \in L^1$ – by applying the inverse Fourier transform and dividing by the dampening factor $e^{\alpha k}$.

Theorem 4.10 (Carr and Madan (1999) Call Option Price)**.** *The t_0-price of a call with strike K and maturity T is given by*

$$\frac{e^{-\alpha\ln(K)}}{2\pi}\int_0^\infty \psi_T(\theta) e^{-i\theta\ln(K)} d\theta. \tag{4.13}$$

Using the FFT method to compute vanilla options improved on the speed of convergence over the quadrature based methods that would be used to compute the integrals in equation 4.12. The computation of vanilla options using characteristic function methods was further improved through the development of the Fang and Oosterlee (2008) COS-method.

4.3.2 Fang and Oosterlee (2008) COS Method

The one dimensional COS method is derived in a similar manner to that of the two dimensional version described in section 6.1. Since this is discussed in depth in a later section, the current section will state results without derivation or detailed discussion. Start with the basic pricing formula

$$v(t_0,x) = e^{-rT}\mathbb{E}^{\mathbb{Q}}\left[v(y,T)|x\right] = e^{-rT}\int_{\mathbb{R}} v(y,T)f(y|x)dy, \tag{4.14}$$

where x is the current log-asset value, y is the log-asset value at time T, $f(y|x)$ is the conditional density function of the final log-asset price given the current log-asset price at time zero. r is the risk-free rate and T the time to maturity and the expectation refers to the conditional expectation under the risk-neutral measure. Then proceed with a series of truncation and expansions which ultimately results in the following COS formula for general underlying processes:

$$V(t_0,x) = e^{-rT}\sum_{n=0}^{N-1}{}' \operatorname{Re}\left\{\phi_T\left(\frac{n\pi}{b-a}\right)e^{in\pi\frac{a}{b-a}}\right\}v_n \tag{4.15}$$

where

$$v_n = \frac{2}{b-a}\int_a^b v(y)\cos\left(n\pi\frac{y-a}{b-a}\right)dy. \tag{4.16}$$

A useful note of the above is that the COS formula compartmentalises the valuation of the derivative into two parts: the payoff specific part in equation 4.16 and the process component as the rest of equation 4.15. This turns the computation of prices of different derivatives under different dynamics into a matter of simple substitution.

For vanilla calls and puts Fang and Oosterlee (2008) prove the result below for Cosine series coefficients needed for equation 4.16 with vanilla options:

Theorem 4.11 (Cosine Series Coefficients for Vanilla Options)**.** *The Cosine series coefficients of functions $g(s) = e^s$ and $g(s) = 1$ on $[c,d] \subset [a,b]$ are given respectively as*

$$\begin{aligned}
\chi_n(c,d) &= \int_c^d e^s\cos\left(n\pi\frac{y-a}{b-a}\right)dy \\
&= \left[1+\left(\frac{n\pi}{b-a}\right)^2\right]^{-1}\times \\
&\quad \left\{\cos\left(n\pi\frac{d-a}{b-a}\right)e^d - \cos\left(n\pi\frac{c-a}{b-a}\right)e^c + \right. \\
&\quad \left.\frac{n\pi}{b-a}\left[\sin\left(n\pi\frac{d-a}{b-a}\right)e^d - \sin\left(n\pi\frac{d-a}{b-a}\right)e^c\right]\right\}
\end{aligned}$$

and

$$\psi_n(c,d) = \begin{cases} d-c & n=0, \\ \frac{b-a}{n\pi}\left[\sin\left(n\pi\frac{d-a}{b-a}\right) - \sin\left(n\pi\frac{c-a}{b-a}\right)\right] & n>0 \end{cases}.$$

Now setting $s_T = \ln(S_T/K)$ – noting that this differs from the S_T defined for Carr and Madan (1999) pricing – and considering theorem 4.11 the formulae for a vanilla call is given by:

$$\begin{aligned} C_n &= \frac{2}{b-a}\int_0^b K(e^y - 1)\cos\left(n\pi\frac{y-a}{b-a}\right)dy \\ &= \frac{2}{b-a}K\left(\chi_k(0,b) - \psi_k(0,b)\right), \end{aligned}$$

similarly the formula for a vanilla put is given by:

$$P_k = \frac{2}{b-a}K\left(-\chi_n(a,0) + \psi_n(a,0)\right).$$

Chapter 5

Hurd and Zhou (2010) Fast Fourier Transform Method

This method, as with the COS-method, approximates the risk-neutral pricing formula 3.1 using a two dimensional version of the revolutionary method originally developed in Carr and Madan (1999).

5.1 Spreads and FFT

The Hurd and Zhou (2010) method was developed in order to price spread options, which are notoriously difficult to price without the use of Monte Carlo or Cosine methods. The first method employed to price spreads using the FFT is that of Dempster and Hong (2002) which developed a two-dimensional version of the Carr and Madan (1999) formula and then made use of a re-arrangement of the summation terms to approximate the exercise region of a spread in a Riemann-sum. The Hurd and Zhou (2010) method was later introduced and found to be faster than that of the Dempster and Hong (2002) method. Thus, for fair comparison use is made of the faster method in this paper.

5.1.1 Hurd and Zhou (2010) method

The method that was developed by Hurd and Zhou (2010) makes use of the logic of Carr and Madan (1999) along with the (then) novel Fourier representation of the basic spread payoff $C(x_1, x_2) = \max(e^{x_1} - e^{x_2} - 1, 0)$, i.e. the payoff given by equation 3.3 in exponential form ($x_i = \ln(S^i)$) with $K = 1$. The representation is given in the theorem below where $\mathbf{x} = (x_1, x_2)$, $\mathbf{u} = (u_1, u_2)$ and finally $\Gamma(z)$ is the complex gamma function which is defined for $\text{Re}(z) > 0$ as $\Gamma(z) = \int_0^\infty e^{-t} t^{z-1} dt$.

Theorem 5.1. *for any real numbers* $\epsilon = (\epsilon_1, \epsilon_2)$ *where* $\epsilon_2 > 0$ *and* $\epsilon_1 + \epsilon_2 < -1$

$$C(\mathbf{x}) = (2\pi)^{-2} \int\int_{\mathbb{R}^2+i\epsilon} e^{iu\mathbf{x}'} \hat{C}(\mathbf{u}) d\mathbf{u}, \quad \hat{C}(\mathbf{u}) = \frac{\Gamma(i(u_1+u_2)-1)\Gamma(-iu_2)}{\Gamma(iu_1+1)}. \tag{5.1}$$

Proof of 5.1 can be found in Hurd and Zhou (2010).

From this result the logic applied in Carr and Madan (1999) is then followed in order to derive an algorithm in which the pricing formula 3.1 can be employed efficiently. This strategy involves combining the formula 5.1 with the explicit formula for the characteristic function of the underlying process. Both the Black Scholes model and the Variance-Gamma model fall under the categorization of Lévy models which are 1-homogeneous (Joshi, 2001). Thus the "simplifying assumption" of homogeneity in Hurd and Zhou (2010) holds which implies that the following factorization of the characteristic function can be used:

$$\mathbb{E}_{X_0}\left[e^{iuX_T'}\right] = e^{iuX_0'}\phi(u;T), \quad \phi(u;T) := \mathbb{E}_0\left[e^{iuX_T'}\right]. \tag{5.2}$$

Pricing Formula

Expressing the asset price process in log form as $S_t = e^{X_t}$ the pricing formula for the basic spread option can be written

$$\begin{aligned} v_{spread}(t_0, \mathbf{x}) &= e^{r\Delta t}\mathbb{E}^{\mathbb{Q}}\left[\max(e^{x_1} - e^{x_2} - 1, 0)\right] \\ &= \frac{e^{r\Delta t}}{(2\pi)^2} \int\int_{\mathbb{R}^2+i\epsilon} \mathbb{E}_{X_0}\left[e^{iuX_T'}\right] \hat{C}(u) d\mathbf{u} \\ &= \frac{e^{r\Delta t}}{(2\pi)^2} \int\int_{\mathbb{R}^2+i\epsilon} e^{iuX_0'}\phi(u;T)\hat{C}(u) d\mathbf{u} \\ &= \frac{e^{r\Delta t}}{(2\pi)^2} \int\int_{\mathbb{R}^2+i\epsilon} e^{iuX_0'}\phi(u;T)\frac{\Gamma(i(u_1+u_2)-1)\Gamma(-iu_2)}{\Gamma(iu_1+1)} d\mathbf{u}. \end{aligned} \tag{5.3}$$

The calculation of the complex gamma in the formula 5.3 is a non-issue as it can be done by the Lanczos (1964) approximation which was shown to be accurate to 13 significant digits on the complex plane by Godfrey (2001) – whose formulation of the the approximation was used in this paper. The double integrals can be approximated by making use of the two-dimensional FFT as derived in Dempster and Hong (2002), which involves truncation and discretisation of the integrals.

Note that the formula 5.3 is for the specific case where $K = 1$. This can be extended to the general case (where $K > 0$) by making use of the 1-homogeneity property and using a simple scaling of the two initial stock prices as follows:

$$v_{spread}(S_{t_0}^1, S_{t_0}^2, K, T) = K \cdot v_{spread}\left(\frac{S_{t_0}^1}{K}, \frac{S_{t_0}^2}{K}, 1, T\right). \tag{5.4}$$

Numerical Integration

The Hurd and Zhou (2010) method for implementing numerical integration is as follows:

1. The double integral in formula 5.3 is approximated via a double sum with N terms – where N is a power of two – in each sum over the lattice:

   $$\Gamma = \left\{ u(k) = (u(k_1), u(k_2)) | k = (k_1, k_2) \in \{0, ..., N-1\}^2 \right\}, \quad u(k) = -\bar{u} + k\eta$$

   for "appropriate" choices of term number N, lattice spacing η and truncation range $(-\bar{u}, \bar{u})$ such that $\bar{u} := \frac{N\eta}{2}$ discretisation leads to an "acceptable" error.

2. Next choose the initial values $X_0 = \ln(S_0)$ to lie on the reciprocal lattice with with lattice spacings $\eta^* = \frac{2\pi}{N\eta} = \frac{\pi}{\bar{u}}$:

   $$\Gamma^* = \{ x(l) = (x(l_1), x(l_2)) | l = (l_1, l_2) \in 0, ..., N-1 \}^2, \quad x(l) = -\bar{x} + l\eta^*, \quad \bar{x} = \frac{N\eta^*}{2}$$

3. Then for any initial stock prices such that $S_0 = e^{X_0}$ and $X_0 = x(l) \in \Gamma^*$ we then have an approximation formula for the value of the spread given by

   $$v_{spread}(t_0, \mathbf{x}) = \frac{\eta^2 e^{-rT}}{(2\pi)^2} \sum_{k_1=0}^{N-1} \sum_{k_2=0}^{N-1} e^{i(u(k_i)+i\epsilon)x(l)'} \phi(u(k_i) + i\epsilon; T) \hat{P}(u(k_i) + i\epsilon)$$

4. Since the Nyquist relation (Press *et al.*, 1989) holds (i.e.$\eta\eta^* = \frac{2\pi}{N}$) we have that

   $$iu(k)x(l)' = i\pi(k_1 + k_2 + l_1 + l_2) + \frac{2\pi i k l'}{N} \pmod{2\pi i}$$

   and thus can write out the approximate formula as:

   $$\begin{aligned} v_{spread}(t_0, \mathbf{x}) &= (-1)^{l_1+l_2} e^{-rT} \left(\frac{\eta N}{2\pi} \right)^2 e^{-\epsilon x(l)'} \left[\frac{1}{N^2} \sum_{k_1=0}^{N-1} \sum_{k_2=0}^{N-1} e^{\frac{2\pi i k l'}{N}} H(k) \right] \\ &= (-1)^{l_1+l_2} e^{-rT} \left(\frac{\eta N}{2\pi} \right)^2 e^{-\epsilon x(l)'} \left[\text{ifft2}(H) \right](l) \end{aligned} \tag{5.5}$$

   where

   $$H(k) = (-1)^{k_1+k_2} \phi(u(k_i) + i\epsilon; T) \hat{P}(u(k_i) + i\epsilon) \tag{5.6}$$

   and ifft2(H) is an application of the two-dimensional inverse FFT of matrix H.

It is important to note that the choice of N,η and ϵ is not straightforward due to the fact that $\bar{u} = \frac{N\eta}{2}$. Minimising the error involved is non-trivial as it is made up of two components whose minimising requirements may conflict: the truncation error and the discretisation error.

The truncation error can be minimised (if the integrand of the pricing equation 5.3 is negligible outside of the region $[-\bar{u} + i\epsilon_1, \bar{u} + i\epsilon_1] \times [-\bar{u} + i\epsilon_2, \bar{u} + i\epsilon_2]$) by taking $\eta \longrightarrow 0$, $N \longrightarrow \infty$ and keeping $\bar{u}$ constant. The discretisation error on the other hand is minimised by taking $\bar{u} \longrightarrow \infty$, $N \longrightarrow \infty$ and keeping η constant.

5.1.2 Choice of Step Size

Olivares and Cane (2014) created a simple yet very effective algorithm in order to ensure both of the initial asset prices land on the inverse grid Γ^* whilst maintaining the Nyquist relation mentioned above, removing any need for the interpolation methods mentioned in the original Hurd and Zhou (2010) article.

Rather than taking equally sized steps of η along the real plane and η^* along the complex plane, Olivares and Cane (2014) specified step sizes across each axes of each plane corresponding to the 2 different assets – i.e. specifying $\eta^{(1)}$ and $\eta^{*(1)}$ for $S^1_{t_0}$ and $\eta^{(2)}$ and $\eta^{*(2)}$ for $S^2_{t_0}$. Furthermore, one can specify a minimum integration interval $\bar{u}_{min}$ for the complex plane, which allows one to determine the step size with minimum truncation error along with removing the interpolation error since each initial asset price will lie on the grid. Defining for each asset $m = 1, 2$ the initial asset log-price as $X^m_{t_0} = \log(S^m_{t_0}/K)$ – where K is the strike – this paper makes use of the following extended version of Olivares and Cane's algorithm which handles both in- and out-the-money options:

Algorithm 1 Algorithm for determining optimal step size η^m

Select N and $\bar{u}_{min}$
for $m = 1, 2$ **do**
    set $j = 0$
    set $\bar{u}_{test} = 0$
    while $\bar{u}_{test} < \bar{u}_{min}$ **do**
        $j = j + 1$
        if $X_0^m > 0$ **then**
            $u_{test} = \frac{\pi(j - N/2)}{X_0^m}$
        else if $X_0^m < 0$ **then**
            $u_{test} = -\frac{\pi(j - N/2)}{X_0^m}$
        end if
    end while
end for

In most Hurd and Zhou (2010) computations in this paper Algorithm 1 is used to determine the appropriate η-values; however in cases where the strike of the option is close in value to one or both of the original asset prices we have that $X_{t_0}^m = \ln(S_{t_0}^m/K) \approx 0$ and one encounters a situation where the step size on at least one underlying is so large that the discretization error is no longer negligible and the asset price becomes unreliable. These situations are handled separately and require interpolation.

5.2 Rainbow Options and FFT

Though there are several examples of Fourier methods to the pricing of rainbow options in the literature – such as (Meng and Ding, 2013), (Da Fonseca *et al.*, 2007) and (Wang, 2009) – none are concerned with pricing by means of the FFT per se and thus the implementation in this paper serves as the first to the author's knowledge. The lack of implementation could perhaps be attributed to rainbow options' relative lack of use in industry compared to that of spreads, or to the practical issues that are encountered in the implementation that are discussed in chapter 7. That being said, the Hurd and Zhou (2010) method can be applied to a rainbow option if an expression for the Fourier inverse of the payoff function can be found. The Fourier inverse of a rainbow option can be found using the work done in Eberlein *et al.* (2010) where the following is presented for an option dependent on d assets.

Given the definition:

Definition 5.2. 1. Let $f(X_T - s)$ be the payoff of an option at time T where X_T

is an $\mathcal{F}_T$ measurable $\mathbb{R}^d$ random variable where f is a measurable function $f : \mathbb{R}^n \longrightarrow \mathbb{R}^+$ and $s = (s^1, \ldots, s^n) \in \mathbb{R}^n$ where $s^i = -\ln(S_T^i)$

2. $g(x) := e^{\langle R,x\rangle} f(x)$ is the dampened payoff function
3. $\varrho(dx) := e^{\langle x\rangle} P_{X_T}(dx)$ is a measure where P_{X_T} is the law of X_T
4. M_{X_T} is the moment generating function of the random vector X_T and $\phi_{\mathbf{X_T}}$ is the characteristic function.

Under the assumptions:

Assumption 5.3.
1. $g \in L^1$
2. M_{X_T} exists
3. $\varrho \in L^1(\mathbb{R}^d)$

The following formula then gives the option price:

Theorem 5.4. *If the asset price processes are modelled as exponential semi-martingale processes (i.e. $S_t^i = S_0^i \exp(H_t^i$ for $0 \leq t \leq T, 1 \leq i \leq d$) where H^i is a semi-martingale) and the above assumptions hold, then the time-0 price function is given by*

$$\mathbb{V}_f(X; s) = \frac{e^{-\langle R,s\rangle}}{(2\pi)^d} \int_{\mathbb{R}^d} e^{-i\langle u,s\rangle} M_{X_T}(R + iu)\hat{f}(iR - u)du. \tag{5.7}$$

The proof of the above theorem can be found in Eberlein *et al.* (2010) where it is named "Theorem 3.2".

A rainbow option driven by a Lévy process meets the assumptions 5.3 and therefore theorem 5.4 can be used. In order to do so one needs to be able to find the Fourier transform of a rainbow options payoff. The derivation of a formula to which the method of Hurd and Zhou (2010) can be applied is presented below.

5.2.1 Fourier Transform of Rainbow Option Payoff

The Fourier inverse of a general rainbow option can be derived using methods from Eberlein *et al.* (2010), but for simplicity this derivation is done for a rainbow call on the min of two assets i.e. the payoff function is of the form $C(x_1, x_2; K) = \max(\min(S_T^1, S_T^2) - K, 0)$. Which can be expressed in terms of log-assets as:

$$f(\mathbf{x}; K) = (e^{x_1} - K)\mathbb{1}_{\{x_1 > x_2\}}\mathbb{1}_{\{x_2 > k\}} + (e^{x_2} - K)\mathbb{1}_{\{x_2 > x_1\}}\mathbb{1}_{\{x_1 > k\}}, \tag{5.8}$$

where $\mathbb{1}$ is the indicator function.

The integrability of the dampened payoff function is used to get an expression for the Fourier inverse of the payoff function, and so we seek the Fourier transform of the $g(x)$ i.e. $\hat{g}(x)$. For clarity we can separate 5.8 into two parts:

$$f_1(x) = (e^{x_1} - K)\mathbb{1}_{\{x_1>x_2\}}\mathbb{1}_{\{x_2>k\}}$$
$$f_2(x) = (e^{x_2} - K)\mathbb{1}_{\{x_2>x_1\}}\mathbb{1}_{\{x_1>k\}}$$

and similarly, taking α_1 and α_2 as dampening factors, one gets the dampened payoff:

$$g_1(x) = e^{(-\alpha_1 x_1 - \alpha_2 x_2)} f_1(x)$$
$$g_2(x) = e^{(-\alpha_1 x_1 - \alpha_2 x_2)} f_2(x).$$

Now consider $\hat{g_1}(u)$, $u \in \mathbb{R}^2$:

$$\begin{aligned}\hat{g_1}(u) &= \int_{\mathbb{R}^2} e^{(iu_1-\alpha_1)x_1+(iu_2-\alpha_2)x_2}(e^{x_1} - K)\mathbb{1}_{\{x_1>x_2\}}\mathbb{1}_{\{x_2>k\}}dx \\ &= \int_k^\infty \int_{x_1}^\infty e^{(iu_1-\alpha_1)x_1+(iu_2-\alpha_2)x_2}(e^{x_1} - K)dx_2dx_1.\end{aligned}$$

One needs the restriction $\alpha_2 < 0$ to evaluate the inner integral and $\alpha_1 + \alpha_2 > 1$ to evaluate the outer integral:

$$\begin{aligned}\hat{g_1}(u) &= \int_k^\infty e^{(iu_2-\alpha_2)x_1}\left(\frac{e^{(iu_1-\alpha_1+1)x_1} - Ke^{(iu_2-\alpha_2)x_1}}{iu_2 - \alpha_2}\right)dx_1 \\ &= \frac{\left[\frac{e^{(iu_1-\alpha_1+iu_2-\alpha_2+1)x_1}}{iu_1-\alpha_1+iu_2-\alpha_2+1}\right]_k^\infty - K\left[\frac{e^{(iu_1-\alpha_1+iu_2-\alpha_2)x_1}}{iu_1-\alpha_1+iu_2-\alpha_2}\right]_k^\infty}{iu_2 - \alpha_2} \\ &= \frac{1}{iu_2 - \alpha_2}\left[\frac{e^{(iu_1-\alpha_1+iu_2-\alpha_2+1)k}}{iu_1 - \alpha_1 + iu_2 - \alpha_2} - \frac{e^{(iu_1-\alpha_1+iu_2-\alpha_2+1)k}}{iu_1 - \alpha_1 + iu_2 - \alpha_2 + 1}\right] \\ &= \frac{K^{(iu_1-\alpha_1+iu_2-\alpha_2+1)}}{(iu_1 - \alpha_1 + iu_2 - \alpha_2)(iu_1 - \alpha_1 + iu_2 - \alpha_2 + 1)} \times \frac{1}{iu_2 - \alpha_2}.\end{aligned}$$

Now consider $\hat{g}(u) = \hat{g_1}(u) + \hat{g_2}(u)$

$$\begin{aligned}\hat{g}(u) &= \frac{K^{(iu_1-\alpha_1+iu_2-\alpha_2+1)}}{(iu_1 - \alpha_1 + iu_2 - \alpha_2)(iu_1 - \alpha_1 + iu_2 - \alpha_2 + 1)} \times \frac{1}{iu_2 - \alpha_2} \\ &+ \frac{K^{(iu_1-\alpha_1+iu_2-\alpha_2+1)}}{(iu_1 - \alpha_1 + iu_2 - \alpha_2)(iu_1 - \alpha_1 + iu_2 - \alpha_2 + 1)} \times \frac{1}{iu_1 - \alpha_1} \\ &= \frac{K^{(iu_1-\alpha_1+iu_2-\alpha_2+1)}}{(iu_1 - \alpha_1 + iu_2 - \alpha_2)(iu_1 - \alpha_1 + iu_2 - \alpha_2 + 1)} \times \left[\frac{1}{iu_1 - \alpha_1} + \frac{1}{iu_2 - \alpha_2}\right] \\ &= \frac{K^{1+\sum_{j=1}^2(iu_j-\alpha_j)}}{\left(1 + \sum_{j=1}^2(iu_j - \alpha_j)\right)\prod_{j=1}^2(iu_j - \alpha_j)}.\end{aligned}$$

From this let $z_j = i(\imath\alpha_j + u_j), \in \mathbb{C}^2$ where $Im(z_j) < 0$ and . The expression for the inverse Fourier Transform of the payoff function can then be put as:

$$\hat{f}(z) = \frac{-K^{1+iz_1+iz_2}}{(1+iz_1+iz_2)(iz_1)(iz_2)}. \tag{5.9}$$

This inverse formula can then be used as the $\hat{C}(u)$ expression in the pricing formula 5.3, which can in turn be approximated using the same Hurd and Zhou (2010) FFT-methodology used to price spreads, which is discussed in Section 5.1.1. When applying this methodology to worst-of options one must abide by the restrictions $\epsilon_1 + \epsilon_2 < -1$ and $\epsilon_1, \epsilon_2 < 0$.

Chapter 6

2D-COS formula for European Options

This section focuses on the derivation of the 2D-COS formula for European options – based on the Fourier-Cosine series of the payoff of the option and the characteristic function of the underlying process – as it was presented in Ruijter and Oosterlee (2012). This formula is ultimately an extension of the COS-method introduced in Fang and Oosterlee (2008) and briefly discussed in section 4.3.2. As mentioned then, this section drills down into the details of how the formula is derived.

Set $T > 0$ to be the finite terminal time at which the option expires. Let $(\Omega, \mathcal{F}, P)$ be a probability space, $\mathbb{F} = (\mathcal{F}_{0 \leq s \leq T})$ be the corresponding filtration satisfying the usual conditions and $\mathbf{X}_t = \left(X_t^1, X_t^2\right)$ be the 2D stochastic process representing the strike-scaled log-asset prices – i.e. $X_t^i = \ln(S_t^i/K)$ where S_t^i is the stock price and K the strike of the option. The price of a European option with payoff $v(T, \mathbf{y})$ is then given by the usual risk-neutral option pricing formula defined by equation 3.1 and restated here for reference:

$$v(t_0, \mathbf{x}) = e^{-r\Delta t}\mathbb{E}_{\mathbb{Q}}^{t_0,\mathbf{x}}\left[v(T, \mathbf{y})\right] = e^{-r\Delta t}\int\int_{\mathbb{R}^2} v(T, \mathbf{y}) f(\mathbf{y}|\mathbf{x}) d\mathbf{y}. \tag{6.1}$$

6.1 Formula Derivation

In order to obtain the formula desired three approximations are applied to formula 6.1 – each of which introduce errors into the final result. For an in depth analysis of the effect of the individual approximations on the overall error in the option value consult Ruijter and Oosterlee (2012).

In the following derivation we make use of the Fourier transform pair linking the conditional density function $f(\mathbf{y}|\mathbf{x})$ to the conditional characteristic function –

as was discussed in section 4.1.1:

$$f(\mathbf{y}|\mathbf{x}) = \left(\frac{1}{2\pi}\right)^2 \int\int_{\mathbb{R}^2} e^{-i\mathbf{u}\cdot\mathbf{y}} \phi(\mathbf{u}|\mathbf{x}) d\mathbf{u} \tag{6.2}$$

$$\phi(\mathbf{u}|\mathbf{x}) = \int\int_{\mathbb{R}^2} e^{i\mathbf{u}\cdot\mathbf{y}} f(\mathbf{y}|\mathbf{x}) d\mathbf{y}. \tag{6.3}$$

Furthermore we make use of the usual shorthand

$$\sum_{k=0}^{N}{}' G_k := \frac{1}{2}G_0 + \sum_{k=1}^{N} G_k.$$

Lastly, this paper adopts the notation of Ruijter and Oosterlee (2012) wherein successive approximations of the option value v are denoted v_i and the final approximation given as $\hat{v}$.

1. The initial step involves the truncation of the integral in formula 6.1. Making the assumption that the integrand of formula 6.1 is integrable we can truncate the domain of integration to $[a_1, b_1] \times [a_2, b_2] \in \mathbb{R}^2$ without significant loss of accuracy, yielding:

$$v_1(t_0, \mathbf{x}) = e^{-r\Delta t} \int_{a_1}^{b_1} \int_{a_2}^{b_2} v(T, \mathbf{y}) f(\mathbf{y}|\mathbf{x}) d\mathbf{y}. \tag{6.4}$$

2. From here we can make use of the two-dimensional Fourier cosine series i.e. the two dimensional version of equations 4.8 and 4.9. Applying the 2D Fourier-Cosine series to $f(\mathbf{y}|\mathbf{x})$ we get:

$$f(\mathbf{y}|\mathbf{x}) = \sum_{k_1=0}^{\infty}{}' \sum_{k_2=0}^{\infty}{}' A_{k_1,k_2}(\mathbf{x}) \cos\left(k_1\pi\frac{y_1 - a_1}{b_1 - a_1}\right) \cos\left(k_2\pi\frac{y_2 - a_2}{b_2 - a_2}\right) \tag{6.5}$$

where $\{A_{k_1,k_2}(\mathbf{x})\}_{k_1,k_2}$ are the cosine series coefficients which are defined:

$$A_{k_1,k_2} := \frac{2}{b_1 - a_1}\frac{2}{b_2 - a_2} \int_{a_1}^{b_1} \int_{a_2}^{b_2} f(\mathbf{y}|\mathbf{x}) \cos\left(k_1\pi\frac{y_1 - a_1}{b_1 - a_1}\right) \cos\left(k_2\pi\frac{y_2 - a_2}{b_2 - a_2}\right) d\mathbf{y}. \tag{6.6}$$

To simplify notation define $k_j^* := \frac{k_j\pi}{b_j - a_j}$ and $\omega_j = \frac{2}{b_j - a_j}$ for $j = 1, 2$. Substitute into 6.4 to get:

$$v_1(t_0, \mathbf{x}) = e^{-r\Delta t} \int_{a_1}^{b_1} \int_{a_2}^{b_2} v(T, \mathbf{y}) \sum_{k_1=0}^{\infty}{}' \sum_{k_2=0}^{\infty}{}' A_{k_1,k_2}(\mathbf{x}) \cos\left(k_1^*(y_1 - a_1)\right) \cos\left(k_2^*(y_2 - a_2)\right) d\mathbf{y}.$$

By interchanging summation and integration we get

$$v_1(t_0, \mathbf{x}) = (\omega_1\omega_2)^{-1} e^{-r\Delta t} \sum_{k_1=0}^{\infty}{}' \sum_{k_2=0}^{\infty}{}' A_{k_1,k_2}(\mathbf{x}) V_{k_1,k_2}(T)$$

where

$$V_{k_1,k_2}(T) := \omega_1\omega_2 \int_{a_1}^{b_1}\int_{a_2}^{b_2} v(T,\mathbf{y}) \cos\left(k_1^*(y_1 - a_1)\right) \cos\left(k_2^*(y_2 - a_2)\right)$$

which are the series coefficients of the truncated version of $v(T, \mathbf{y})$.

3. Having introduced the Fourier-cosine series the summations are now made computable by truncating them down to the sum of the first N_1 and N_2 terms respectively. This yields the next price approximation:

$$v_2(t_0, \mathbf{x}) = (\omega_1\omega_2)^{-1} e^{-r\Delta t} \sum_{k_1=0}^{N_1-1}{}' \sum_{k_2=0}^{N_2-1}{}' A_{k_1,k_2}(\mathbf{x}) V_{k_1,k_2}(T). \tag{6.7}$$

4. Now that the series summation has been dealt with, one needs to consider the cosine series coefficients A_{k_1,k_2} which need to be approximated. By "reversing" the truncation in step 1, we get an approximation for A_{k_1,k_2}:

$$F_{k_1,k_2}(\mathbf{x}) := \omega_1\omega_2 \int\int_{\mathbb{R}^2} f(\mathbf{y}|\mathbf{x}) \cos\left(k_1^*(y_1 - a_1)\right) \cos\left(k_2^*(y_2 - a_2)\right) d\mathbf{y}. \tag{6.8}$$

Making use of the trigonometric identity below

$$2\cos(\alpha)\cos(\beta) = \cos(\alpha + \beta) + \cos(\alpha - \beta),$$

one can manipulate equation 6.8 as follows:

$$\begin{aligned}
F_{k_1,k_2} &= \omega_1\omega_2 \int\int_{\mathbb{R}^2} f(\mathbf{y}|\mathbf{x}) \cos\left(k_1^*(y_1 - a_1)\right) \cos\left(k_2^*(y_2 - a_2)\right) d\mathbf{y} \\
&= \omega_1\omega_2 \int\int_{\mathbb{R}^2} f(\mathbf{y}|\mathbf{x}) \frac{1}{2}[\cos(k_1^*(y_1 - a_1) + k_2^*(y_2 - a_2)) \\
&\quad + \cos(k_1^*(y_1 - a_1) - k_2^*(y_2 - a_2))] d\mathbf{y} \\
&= \frac{1}{2}\omega_1\omega_2 \left[\int\int_{\mathbb{R}^2} f(\mathbf{y}|\mathbf{x}) \cos(k_1^*(y_1 - a_1) + k_2^*(y_2 - a_2)) d\mathbf{y} \right. \\
&\qquad \left. \int\int_{\mathbb{R}^2} f(\mathbf{y}|\mathbf{x}) \cos(k_1^*(y_1 - a_1) - k_2^*(y_2 - a_2)) d\mathbf{y}\right] \\
&= \frac{1}{2}\left[F^+_{k_1,k_2}(\mathbf{x}) + F^-_{k_1,k_2}(\mathbf{x})\right]
\end{aligned}$$

where

$$F^{\pm}_{k_1,k_2} := \omega_1\omega_2 \int\int_{\mathbb{R}^2} f(\mathbf{y}|\mathbf{x}) \cos(k_1^*(y_1 - a_1) \pm k_2^*(y_2 - a_2)) d\mathbf{y} \tag{6.9}$$

The $F^{\pm}_{k_1,k_2}$ coefficients given by 6.9 can be expressed using the characteristic function – using Euler's Formula – as defined in formula 6.3 as follows:

$$\begin{aligned} F^{\pm}_{k_1,k_2} &= \omega_1\omega_2 \text{Re}\left(\int\int_{\mathbb{R}^2} f(\mathbf{y}|\mathbf{x}) \exp[(ik_1^*(y_1-a_1) \pm ik_2^*(y_2-a_2))] d\mathbf{y}\right) \\ &= \omega_1\omega_2 \text{Re}\left(\int\int_{\mathbb{R}^2} f(\mathbf{y}|\mathbf{x}) \exp[(ik_1^* y_1 \pm ik_2^* y_2] d\mathbf{y} \exp[-ik_1^* a_1 \mp ik_2^* a_2]\right) \\ &= \omega_1\omega_2 \text{Re}\left(\phi(k_1^*, \pm k_2^*|\mathbf{x}) \exp[-ik_1^* a_1 \mp ik_2^* a_2]\right) \end{aligned}$$

which for Lévy processes in particular, since $\phi_{levy}(u_1,u_2) := \phi(u_1,u_2|0,0)$, can be expressed with an unconditional characteristic function.

$$F^{\pm}_{k_1,k_2} = \omega_1\omega_2 \text{Re}\left(\phi_{levy}(k_1^*, \pm k_2^*) \exp[ik_1^*(x_1-a_1) \mp ik_2^*(x_2-a_2)]\right). \quad (6.10)$$

Finally by inserting 6.10 into 6.7 we get an approximation of $v(t_0,\mathbf{x})$ as:

$$\hat{v}(t_0,\mathbf{x}) := (\omega_1\omega_2)^{-1} e^{-r\Delta t} \sum_{k_1=0}^{N_1-1\prime} \sum_{k_2=0}^{N_2-1\prime} \frac{1}{2}\left[F^{+}_{k_1,k_2}(\mathbf{x}) + F^{-}_{k_1,k_2}(\mathbf{x})\right] V_{k_1,k_2}(T). \quad (6.11)$$

6.2 Computational Domain

The importance of the choice of how to truncate the domain of integration from $\mathbb{R}^2$ to $[a_1,b_1]\times[a_2,b_2]$ must not be underestimated when dealing with the 2D-COS method as a "trade-off" between speed and accuracy must be undertaken: using too small a domain could result in serious inaccuracies, whilst larger domains require a greater number of expansion terms in order to yield a particular accuracy. Since this paper uses both speed and accuracy in order to determine the efficiency of the two methods, it is clear that this truncation of the domain holds a great deal of weight.

Following the methodology of Ruijter and Oosterlee (2012) equal domains for each dimension are taken in order to simplify computations. So $a_1 = a_2 = a$ and $b_1 = b_2 = b$ where

$$a := \min_i \left[x_0^i + c_1^i - L\sqrt{c_2^i + \sqrt{c_4^i}}\right], \quad b := \min_i \left[x_0^i + c_1^i + L\sqrt{c_2^i + \sqrt{c_4^i}}\right] \quad (6.12)$$

where $L = 10$, and c_j^i is the jth cumulant of the random variable X_t^i – which in turn is defined as $X_t^i := \ln \frac{S_t^i}{K}$ where S_t^i is the stock price of asset i and K is the strike of the derivative.

Since the choice of computational domain is possibly the most important element of the method when it comes to accuracy, a test of the robustness of the COS-method with respect to changes in the computational domain is presented later in the paper in section 7.2.2.

6.3 Computing the V_{k_1,k_2} Terms

For European vanilla options the V_{k_1,k_2} can be expressed in a closed form, however in two or more dimensional problems only exceptions such as Magrabe options or geometric basket options offer explicit formulae. In the case of rainbow and spread options there is in general no closed expression for these series coefficients, thus we approximate them using the inverse of the *Type II discrete cosine transforms* (DCTs) discussed in section 4.2.1. For notes about higher-order problems and convergence of errors introduced by approximating V_{k_1,k_2} refer to Ruijter and Oosterlee (2012)

6.3.1 Discrete Cosine Transform

In order to approximate the V_{k_1,k_2} terms from equation 6.11 we use the rectangle method of numerical integration on the double definite integral. Taking $Q \geq \max[N_1, N_2]$ grid-points for each dimension we then define the grid-points and the grid-steps for $i = 1, 2$ as:

$$y_i^{n_i} := a_i + \left(n_i + \frac{1}{2}\right)\frac{b_i - a_i}{Q} \qquad \text{and} \qquad \Delta y_i := \frac{b_i - a_i}{Q}.$$

When applying the rectangle method using the mid-points it yields

$$\begin{aligned} V_{k_1,k_2}(T) &\approx \omega_1\omega_2 \sum_{n_1=0}^{Q-1}\sum_{n=0}^{Q-1} v(T, y_1^{n_1}, y_2^{n_2}) \cos(k_1^*(y_1^{n_1} - a_1)) \cos(k_2^*(y_2^{n_2} - a_2))\Delta y_1 \Delta y_2 \\ &= \sum_{n_1=0}^{Q-1}\sum_{n=0}^{Q-1} v(T, y_1^{n_1}, y_2^{n_2}) \cos\left(k_1\pi\frac{2n_1+1}{2Q}\right) \cos\left(k_2\pi\frac{2n_2+1}{2Q}\right)\frac{4}{Q^2}. \end{aligned}$$

Which can be seen to be the two dimensional inverse DCT given in equation 4.11.

Chapter 7

Results

7.1 Speed of Convergence

The parameters used for the Black-Scholes and Variance-Gamma models in this section are taken from Dempster and Hong (2002) and Kienitz and Wetterau (2012) respectively:

Tab. 7.1: Model parameters

	Black-Scholes	Variance-Gamma
Parameters	$\underline{\sigma} = (0.1, 0.2)$	$\underline{\sigma} = (0.1, 0.2)$
	$\rho = 0.5$	$\rho = 0.5$
	$\underline{\delta} = (0.05, 0.05)$	$\underline{\delta} = (0.05, 0.05)$
		$\underline{\theta} = (-0.6094, -0.8301)$
		$\nu = 0.2570$

The common parameters are the risk-free rate $r = 0.1$, and the time to maturity $T = 1$.

Furthermore for the COS method we take $a_1 = a_2 = a$, $b_1 = b_2 = b$, $N1 = N2 = N$ and $Q = 2000$ in line with Ruijter and Oosterlee (2012) and for the FFT method, we use $[\epsilon_1, \epsilon_2] = [-3, 1]$ for spreads, in line with what was used in Hurd and Zhou (2010), and $[\epsilon_1, \epsilon_2] = [-3, -1]$ for the worst-of rainbow options.

For simplicity this paper first considers the prices found under each method using the standard Black- Scholes stock price model, as accurate closed form approximations exist against which we can compare. Then the Variance-Gamma model is considered and the same analysis is performed.

7.1.1 Spread Options

For spread options we take initial stock prices of $S_0 = (100, 96)$ and strikes between 0.5 and 4 in half unit increments and compute the prices using the Hurd and Zhou (2010) FFT- and COS- methodology and for comparison we compute the Monte-Carlo price using a sample size of five million – the results of which can are presented in Table A.1 for the Black-Scholes model and Table A.6 for the Variance-Gamma model. For the Black-Scholes model we also compute the Bjerksund-Stensland approximation for comparison as it has been shown to be highly accurate – for elaboration refer to the original article Bjerksund and Stensland (2014).

Black-Scholes Model

Using the methodology of Hurd and Zhou (2010) along with Algorithm 1, as well as the straightforward two-dimensional cosine methodology under GBM gives the FFT- and COS-method prices which can be seen in full in Tables A.2 and A.4 respectively. This is repeated for values of $N = 2^n, n = 4, 5, 6, ..., 10$ in order to gauge the rate of convergence. As can be seen in Table A.3 versus Table A.5 the FFT-estimate converges to three decimal places – to the Bjerksund-Stensland price – for all strikes after 128 terms are included in the summation, whereas the COS-estimate converges after 32 terms as can be seen in figure 7.1.

Fig. 7.1: Comparison of the FFT and COS convergence for GBM spread options

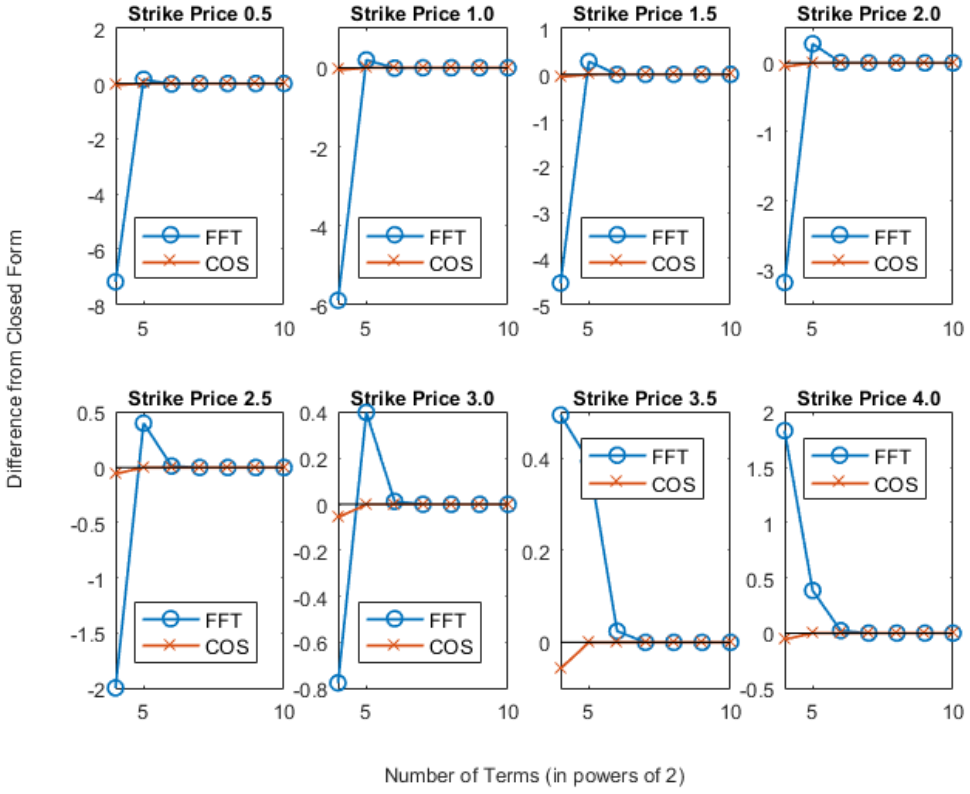

Thus, the price of a spread option under GBM converges quicker for the Ruijter and Oosterlee (2012) COS-method than the Hurd and Zhou (2010) FFT-method.

Variance-Gamma Model

Making use of the same methodology as above but using the VG model instead, we firstly get the relevant Monte-Carlo estimates (based on 5 million simulation) and their standard deviations – the results of which can are presented in Table A.9 for the Black-Scholes model and Table A.14 for the Variance-Gamma model. Since closed form solutions do not exist for spread prices under the Variance-Gamma model, these are used as a guide for what expected prices should be using the other methods. This paper also makes use of the fact that the likelihood of the actual option price differing from the Monte Carlo estimate by more than three standard deviations is almost zero as a determinant of the level of convergence of prices. This method is used in the determination of convergence for the VG model as there is no closed-form against which to compare the price estimates.

Tab. 7.2: Monte Carlo Variance-Gamma spread prices and standard deviations

Monte-Carlo Spread Option Prices and Standard Deviations								
	0.5	**1**	**1.5**	**2**	**2.5**	**3**	**3.5**	**4**
Price	8.2039	7.9245	7.6498	7.3797	7.1145	6.8541	6.5986	6.3481
SD	0.0046	0.0045	0.0044	0.0044	0.0043	0.0041	0.0041	0.0040

The same methodology as above is used except the Variance-Gamma model is substituted in the place of GBM. Comparing the results in Table A.7 and Table A.8 along with the Monte Carlo estimates and standard deviations through the 3 standard deviation bound mentioned above one can see the convergence in the figure 7.2:

Fig. 7.2: Comparison of the FFT and COS convergence for VG spread options

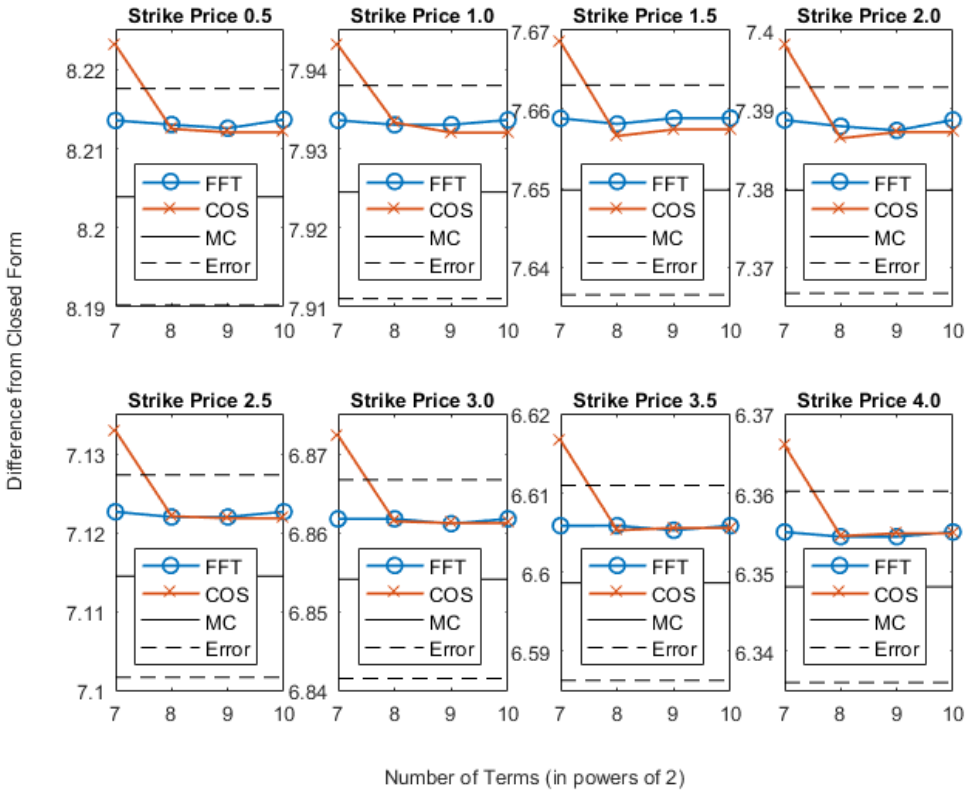

Here we see that under the VG model the COS estimates converge to within the error bounds after the inclusion of 256 terms, whereas the FFT estimates converge after the inclusion of 128 terms.

Under initial examination one could quickly conclude that the price of a spread option under VG converges quicker for the Hurd and Zhou (2010) FFT-method than the Ruijter and Oosterlee (2012) COS-method; however since for the COS-method the value of N need not be a power of two, the convergence of the price to within the error bounds could occur for a value of N between 128 and 256. In examining this it can be seen that the COS method prices begin to lie within the error bounds after the inclusion of 130 terms, which is insubstantially different from the 128 needed for convergence of the FFT estimate – Thus one can conclude that the prices converge at a similar rate. It is worth noting that both types of estimates are converging to similar values.

7.1.2 Rainbow Options

Here again initial stock prices of $S_0 = (100, 96)$ are taken, however the strike prices now range between 90 and 104 in increments of two. Again, the prices are computed using the Hurd and Zhou (2010) FFT- and COS- methodology and then for comparison we compute the Monte-Carlo prices – full results can be seen in Tables A.10, A.12 and A.9 respectively. Here for the Black-Scholes model we also compute the Stulz (Stulz, 1982) approximation for comparison.

Black-Scholes Model

Following a similar outline to the results for spread options in section 7.1.1 we now compute the corresponding FFT prices; however when it comes to worst-of rainbow options that are around at-the-money (ATM), the Algorithm 1 produces step sizes (along at least one of the dimensions, more specifically the dimension where $X_t^i \approxeq 0$) that are so large that the discretization error introduced by the approximation of the double integral increases drastically leading to highly inaccurate results. Thus, for options around ATM (in this case those with strikes of 96,98 and 100) one needs to revert back to a single selection of step size and interpolation. In this paper cubic - spline interpolation is used. The related results tables (namely tables A.10 and A.15) thus includes the values of $\bar{u}$ for the affected option prices. The values $\bar{u}$ are chosen to try and incur minimal truncation errors across all strikes – error plots in appendix B.1 show how the truncation error changes for a strike of 98. One can note that no single $\bar{u}$ works consistently well across all values of N, so unlike in Hurd and Zhou (2010) it is not possible to determine an optimal $\bar{u}$ to use. This causes an issue of circularity in the results where one needs an estimate of the price in order to choose an appropriate $\bar{u}$ in order to estimate the price – this is clearly problematic.

Comparing the two relevant tables, Tables A.11 and A.13, we get that with the exception of the strike of 90 – which does not converge to three decimal places at all – all other FFT-prices converge to three decimal places after 512 terms are included, convergence to the third decimal place with the COS-method occurs after 64 terms are included.

Fig. 7.3: Comparison of the FFT and COS convergence for GBM rainbow options

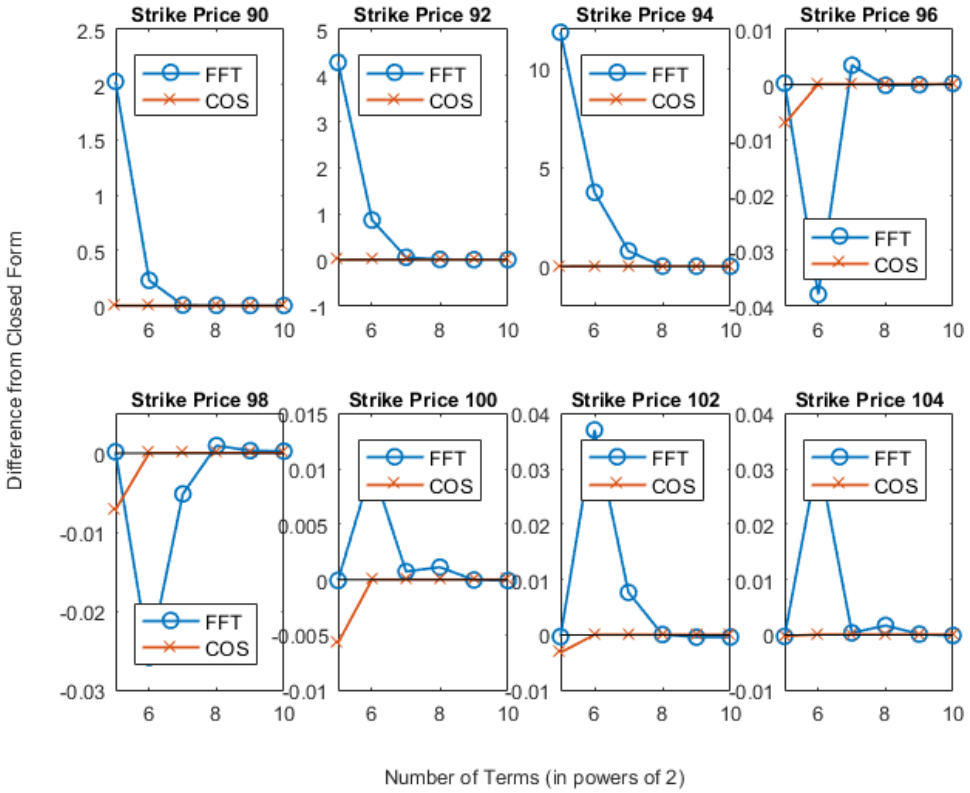

Thus we get a similar result to that of the spread options under GBM where the convergence is faster for the COS-method than the FFT-method; furthermore, for the strike of 90 the COS method is simply more accurate across all values of N in this paper. This result could bring into question the accuracy of the FFT-method for further in-the-money (ITM) rainbow options – further investigation into this is necessary in order to make any definitive conclusions.

Variance-Gamma Model

Again under the VG model we make use of Monte Carlo estimates and the estimates'standard deviations – as no closed form price exists – as a measure for con-

vergence.

Tab. 7.3: Monte Carlo Variance-Gamma rainbow option prices and standard deviations

	Monte-Carlo Rainbow Option Prices and Standard Deviations							
	90	**92**	**94**	**96**	**98**	**100**	**102**	**104**
Price	15.705	14.705	13.741	12.814	11.925	11.071	10.256	9.4776
SD	0.0097	0.0094	0.0091	0.0087	0.0084	0.0081	0.0078	0.0074

We encounter a similar issue to GBM with the VG model when it comes to the calculation of step size for the FFT-price, except that it is more pronounced. Here only deep in-the-money (ITM) and out-the-money (OTM) options can be done without interpolation, so the FFT results here again use a single $\bar{u}$ value is chosen and cubic interpolation is used. The choice of $\bar{u}$ here made use of the Monte Carlo estimate to determine the truncation error to minimise, which again presents very obvious issues when it comes to practical implementation.

Comparing the two relevant tables (Tables A.15 and A.16) as well as the Monte Carlo estimates and error bounds we see that the FFT method converges after 64 terms and the COS method prices after 128.

Fig. 7.4: Comparison of the FFT and COS convergence for VG rainbow options

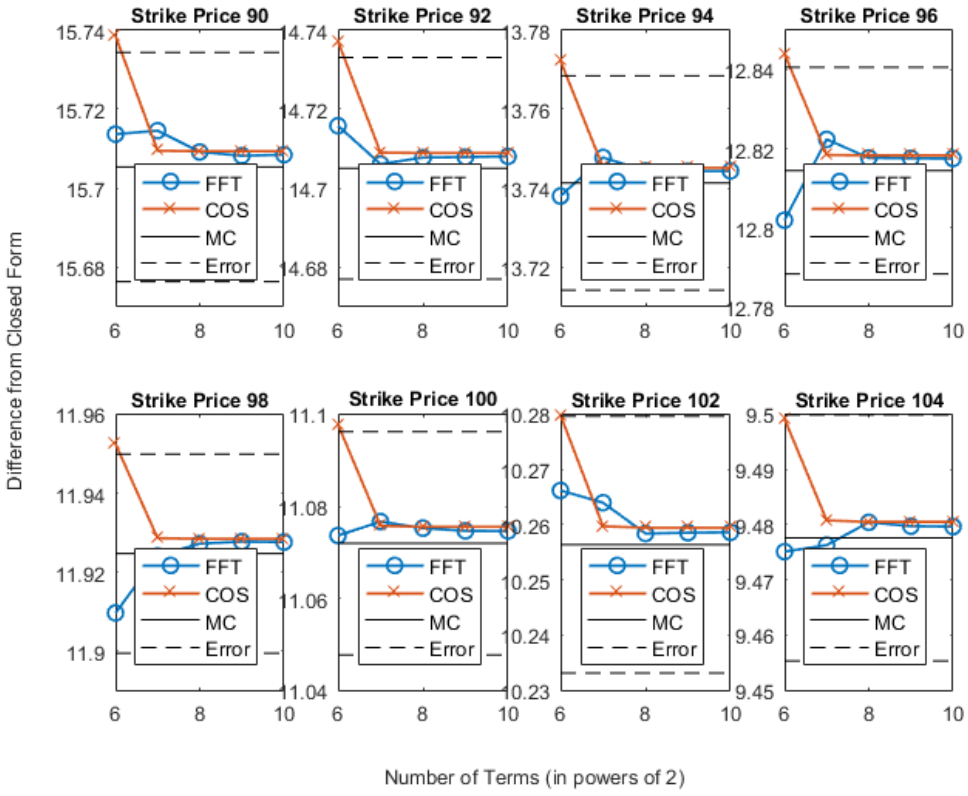

Again the case of an N value which is not a power of 2 can be considered for the COS estimates, and the estimates converge after the inclusion of 66 which is not significantly different from the 64 terms that it takes the FFT method prices to converge. Thus it can be concluded that the FFT and COS methods converge at a similar rate for rainbow option prices modelled using the Variance-Gamma model.

7.2 Robustness of Methods

The following section considers the robustness of each method to their various "discretionary" choice variables – namely the ϵ- values for the Hurd and Zhou (2010) FFT method and the Q- and L-values for the Ruijter and Oosterlee (2012) COS method.

This paper considers the results under the GBM model as there exists closed form solutions against which to compare. The effect on both spreads and rainbow options is considered.

7.2.1 Fast Fourier Transform Robustness

Considering the robustness of the spread option price, we set $K = 2$, $N = 512$, and $\bar{u}_{min} = 20$. We then consider ϵ- values from -7 to 5.5 in increments of a half ensuring that they adhere to the restrictions that $\epsilon_1 < 0$ and $\epsilon_1 + \epsilon_2 < -1$. Which gives the following:

Tab. 7.4: Spread option prices under GBM with varying ϵ_1 and ϵ_2

Spread Option Prices Under varying ϵ - Values												
							ϵ_1					
		-2	**-2.5**	**-3**	**-3.5**	**-4**	**-4.5**	**-5**	**-5.5**	**-6**	**-6.5**	**-7**
ϵ_2	**0.5**	7.542331	7.542244	7.542156	7.542068	7.541974	7.541848	7.541644	7.541361	7.541527	7.545643	7.571520
	1		7.542235	7.542156	7.542089	7.542036	7.541983	7.541887	7.541632	7.541003	7.539817	7.539433
	1.5			7.542144	7.542083	7.542049	7.542041	7.542043	7.541998	7.541738	7.540832	7.538298
	2				7.542069	7.542035	7.542041	7.542085	7.542152	7.542179	7.541969	7.540929
	2.5					7.542021	7.542021	7.542071	7.542170	7.542303	7.542417	7.542317
	3						7.542009	7.542047	7.542140	7.542288	7.542482	7.542686
	3.5							7.542039	7.542115	7.542245	7.542430	7.542668
	4								7.542112	7.542222	7.542379	7.542582
	4.5									7.542227	7.542374	7.542528
	5										7.542374	7.542520
	5.5											7.542542

Tab. 7.5: Spread option price deviations from Bjerksund and Stensland approximation with varying ϵ_1 and ϵ_2

Spread Option Price Deviations From Closed-Form Under Varying ϵ - Values												
							ϵ_1					
		-2	**-2.5**	**-3**	**-3.5**	**-4**	**-4.5**	**-5**	**-5.5**	**-6**	**-6.5**	**-7**
ϵ_2	**0.5**	0.000009	-0.000078	-0.000166	-0.000254	-0.000348	-0.000474	-0.000678	-0.00096	-0.000795	0.003321	0.029198
	1		-0.000087	-0.000166	-0.000233	-0.000286	-0.000339	-0.000435	-0.000690	-0.001319	-0.002505	-0.002889
	1.5			-0.000178	-0.000239	-0.000273	-0.000281	-0.000279	-0.000324	-0.000584	-0.001490	-0.004024
	2				-0.000253	-0.000287	-0.000281	-0.000237	-0.000170	-0.000143	-0.000353	-0.001393
	2.5					-0.000301	-0.000301	-0.000251	-0.000152	-0.000019	0.000095	-0.000005
	3						-0.000313	-0.000275	-0.000182	-0.000034	0.000160	0.000364
	3.5							-0.000283	-0.000207	-0.000077	0.000108	0.000347
	4								-0.000210	-0.000100	0.000057	0.000260
	4.5									-0.000095	0.000052	0.000206
	5										0.000052	0.000198
	5.5											0.000220

It can be seen that the option price is relatively insensitive to the changes in epsilon values which mostly only affect the price at the third decimal place. It can be seen that the error level is affected mostly by the differences between the two ϵ-values rather than their individual absolute values – specifically the larger the absolute value of the sum of the two epsilon values, the greater the error tends to be.

Fig. 7.5: Sum of ϵ-values against average absolute errors

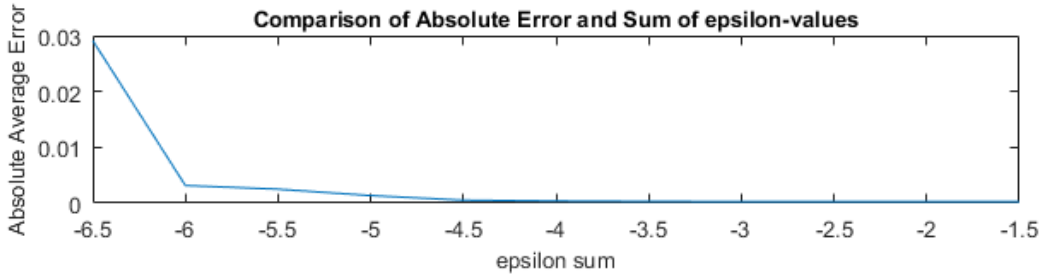

Now considering the worst-of rainbow options with $K = 90$, $N = 512$, and $\bar{u}_{min} = 20$ and ϵ-values ranging from -1 to -10 in unit steps. Again, one needs to keep within the limits on the ϵ-values; namely here $\epsilon_1, \epsilon_2 < 0$ and $\epsilon_1 + \epsilon_2 < -1$.

Tab. 7.6: Rainbow option prices under GBM with varying ϵ_1 and ϵ_2

Rainbow Option Price Under Varying ϵ - Values										
		ϵ_1									
		-1	**-2**	**-3**	**-4**	**-5**	**-6**	**-7**	**-8**	**-9**	**-10**
ϵ_2	**-1**	6.055461	6.055461	6.05546	6.05546	6.05546	6.05546	6.05546	6.05546	6.05546	6.055461
	-2	6.055239	6.055239	6.055238	6.055238	6.055238	6.055238	6.055238	6.055238	6.055238	6.055239
	-3	6.055239	6.055239	6.055238	6.055238	6.055238	6.055238	6.055238	6.055238	6.055238	6.055239
	-4	6.055239	6.055239	6.055238	6.055238	6.055238	6.055238	6.055238	6.055238	6.055238	6.055239
	-5	6.055239	6.055239	6.055238	6.055238	6.055238	6.055238	6.055238	6.055238	6.055238	6.055239
	-6	6.055239	6.055239	6.055238	6.055238	6.055238	6.055238	6.055238	6.055238	6.055238	6.055239
	-7	6.055239	6.055239	6.055238	6.055238	6.055238	6.055238	6.055238	6.055238	6.055238	6.055239
	-8	6.055239	6.055239	6.055238	6.055238	6.055238	6.055238	6.055238	6.055238	6.055238	6.055239
	-9	6.055239	6.055239	6.055238	6.055238	6.055238	6.055238	6.055238	6.055238	6.055238	6.055239
	-10	6.055239	6.055239	6.055238	6.055238	6.055238	6.055238	6.055238	6.055238	6.055238	6.055239

Tab. 7.7: Rainbow option price deviations from Stulz approximation with varying ϵ_1 and ϵ_2

Rainbow Option Price Deviation from Closed-form Under Varying ϵ - Values										
		ϵ_1									
		-1	**-2**	**-3**	**-4**	**-5**	**-6**	**-7**	**-8**	**-9**	**-10**
ϵ_2	**-1**	0.000222	0.000222	0.000222	0.000222	0.000222	0.000221	0.000221	0.000221	0.000222	0.000222
	-2	2.952E-07	1.628E-07	-4.057E-08	-2.861E-07	-5.270E-07	-7.036E-07	-7.520E-07	-6.180E-07	-2.727E-07	2.700E-07
	-3	2.906E-07	1.582E-07	-4.519E-08	-2.907E-07	-5.317E-07	-7.082E-07	-7.566E-07	-6.225E-07	-2.773E-07	2.654E-07
	-4	2.906E-07	1.582E-07	-4.519E-08	-2.907E-07	-5.317E-07	-7.082E-07	-7.566E-07	-6.225E-07	-2.773E-07	2.654E-07
	-5	2.906E-07	1.582E-07	-4.519E-08	-2.907E-07	-5.317E-07	-7.082E-07	-7.566E-07	-6.225E-07	-2.773E-07	2.654E-07
	-6	2.906E-07	1.582E-07	-4.519E-08	-2.907E-07	-5.317E-07	-7.082E-07	-7.566E-07	-6.225E-07	-2.773E-07	2.654E-07
	-7	2.906E-07	1.582E-07	-4.519E-08	-2.907E-07	-5.317E-07	-7.082E-07	-7.566E-07	-6.225E-07	-2.773E-07	2.654E-07
	-8	2.906E-07	1.582E-07	-4.519E-08	-2.907E-07	-5.317E-07	-7.082E-07	-7.566E-07	-6.225E-07	-2.773E-07	2.654E-07
	-9	2.906E-07	1.582E-07	-4.519E-08	-2.907E-07	-5.317E-07	-7.082E-07	-7.566E-07	-6.225E-07	-2.773E-07	2.654E-07
	-10	2.906E-07	1.582E-07	-4.519E-08	-2.907E-07	-5.317E-07	-7.082E-07	-7.566E-07	-6.225E-07	-2.773E-07	2.654E-07

As can be seen, rainbow option prices are highly insensitive with respect to ϵ-

values and for values of ϵ_2 and above the error introduced by the choice in ϵ_1 is inconsequential.

7.2.2 COS Method Robustness

A similar analysis is done for the COS pricing method to test the sensitivity of the prices to the integration truncation range variable L and the DCT truncation variable Q.

For the spread option we again take $K = 2$, $N = 512$ and furthermore take L-values ranging from 1 to 26 in unit steps and Q-values of $N, 600, 700, \ldots, 2900, 3000$ – the odd starting value of this sequence is as a result of the fact that the lowest value that Q can take on is N. The price estimate for each value of L and Q are given in tables 7.8 and 7.9 along with the difference from the Bjerksund and Stensland closed form approximation.

As can be seen, with the exception of the four smallest L and the lowest Q values, the method is robust against differences to the third decimal place. In fact increasing the Q value above 800 has minimal effect on the price and would only really increase the computation time with relatively minimal benefit.

Tab. 7.8: COS method robustness against changes in the L-value

L	Estimate	Difference
1	4.84372351	-2.69859849
2	7.08397669	-0.45834531
3	7.51630946	-0.02601254
4	7.54172974	-0.00059226
5	7.54231847	-0.00000353
6	7.54232388	0.00000188
7	7.54232390	0.00000190
8	7.54232390	0.00000190
9	7.54232389	0.00000189
10	7.54232391	0.00000191
11	7.54232389	0.00000189
12	7.54232388	0.00000188
13	7.54232388	0.00000188
14	7.54232394	0.00000194
15	7.54232385	0.00000185
16	7.54232384	0.00000184
17	7.54232430	0.00000230
18	7.54232359	0.00000159
19	7.54232248	0.00000048
20	7.54232450	0.00000250
21	7.54232793	0.00000593
22	7.54232629	0.00000429
23	7.54231807	-0.00000393
24	7.54231183	-0.00001017
25	7.54231672	-0.00000528
26	7.54233294	0.00001094

Tab. 7.9: COS method robustness against changes in the Q-value

Q	Estimate	Difference
512	7.54252350	0.00020150
600	7.54224744	-0.00007456
700	7.54235044	0.00002844
800	7.54231672	-0.00000528
900	7.54232487	0.00000287
1000	7.54232450	0.00000250
1100	7.54232331	0.00000131
1200	7.54232423	0.00000223
1300	7.54232377	0.00000177
1400	7.54232394	0.00000194
1500	7.54232389	0.00000189
1600	7.54232391	0.00000191
1700	7.54232390	0.00000190
1800	7.54232390	0.00000190
1900	7.54232390	0.00000190
2000	7.54232391	0.00000191
2100	7.54232390	0.00000190
2200	7.54232390	0.00000190
2300	7.54232390	0.00000190
2400	7.54232389	0.00000189
2500	7.54232390	0.00000190
2600	7.54232389	0.00000189
2700	7.54232390	0.00000190
2800	7.54232390	0.00000190
2900	7.54232390	0.00000190
3000	7.54232390	0.00000190

For the rainbow option we similarly take $N = 512$ and L-values ranging from 1 to 26 in unit steps and Q-values of $N, 600, 700, \ldots, 2900, 3000$. We assume $K = 90$ as with the FFT testing and the results are presented in tables 7.10 and 7.11.

Tab. 7.10: COS method robustness against changes in the L-value

L	Estimate	Difference
1	7.29350152	-0.98067447
2	8.25238464	-0.02179135
3	8.27412359	-0.00005240
4	8.27418944	0.00001345
5	8.27418109	0.00000511
6	8.27420406	0.00002808
7	8.27418424	0.00000825
8	8.27423487	0.00005888
9	8.27418799	0.00001200
10	8.27424543	0.00006944
11	8.27429007	0.00011408
12	8.27423566	0.00005968
13	8.27425937	0.00008338
14	8.27432300	0.00014701
15	8.27420286	0.00002687
16	8.27423205	0.00005606
17	8.27441078	0.00023479
18	8.27440636	0.00023037
19	8.27449844	0.00032245
20	8.27436766	0.00019167
21	8.27422315	0.00004716
22	8.27423591	0.00005992
23	8.27430588	0.00012989
24	8.27453341	0.00035742
25	8.27474778	0.00057179
26	8.27474017	0.00056419

Tab. 7.11: COS method robustness against changes in the Q-value

Q	Estimate	Difference
512	8.27556818	0.00139219
600	8.27510363	0.00092764
700	8.27435682	0.00018084
800	8.27474778	0.00057179
900	8.27451777	0.00034179
1000	8.27436766	0.00019167
1100	8.27448862	0.00031263
1200	8.27431273	0.00013674
1300	8.27433715	0.00016116
1400	8.27436357	0.00018758
1500	8.27421783	0.00004184
1600	8.27430505	0.00012907
1700	8.27429161	0.00011562
1800	8.27420267	0.00002669
1900	8.27427730	0.00010131
2000	8.27424543	0.00006944
2100	8.27421910	0.00004311
2200	8.27425414	0.00007815
2300	8.27421352	0.00003753
2400	8.27422307	0.00004708
2500	8.27423487	0.00005888
2600	8.27419025	0.00001426
2700	8.27422120	0.00004521
2800	8.27421871	0.00004272
2900	8.27418599	0.00001000
3000	8.27421658	0.00004059

The COS-method rainbow option prices seem to be less robust against changes in the L and Q values, although again with the exception of the first three L-values and the first Q-value the rest are robust up to three decimal places.

Chapter 8

Conclusion

As markets become more developed, the need for a fast and accurate method of pricing more complex financial options becomes more pressing. Thus, this paper serves to compare two of the main Fourier pricing methods in terms of convergence rates and robustness – namely Hurd and Zhou's fast Fourier transform method and Ruijter and Oosterlee's cosine series expansion method.

It was found that although the COS method converged faster than the FFT method when modelling under the Black-Scholes model for both spread options (32 versus 128 terms) and the rainbow options (64 versus 512 terms) this was not the case when the underlying model was changed to the more complex Variance-Gamma model. Under the VG model the rate of convergence for the COS and FFT method is fairly similar – specifically convergence occurs, respectively, for spread options within 130 and 128 terms and for rainbow options within 66 and 64 terms.

The robustness of the pricing methodologies to changes in discretionary variables was also considered for options in the Black-Scholes world. In general both the COS and FFT methods were found to be robust in general, with the exception of the application of the FFT method to rainbow options. A serious practical limitation was found where the choice of truncation region heavily affected the prices of the worst-of options across varying numbers of series terms; thus not one single truncation parameter could be indiscriminately used.

In conclusion this paper finds that for practical purposes, the COS method is preferable for pricing spread and rainbow options under GBM and VG models due to its similar speed and greater robustness than the FFT method. Further studies into the effect of increasingly complex models and other exotic options are suggested in order to determine a more complete picture of the effectiveness of each method. Furthermore, an investigation into the practical limitation of the application of the FFT method to rainbow options – discussed in Chapter 7 should be conducted.

Bibliography

Barndorff-Nielsen, O. E., Mikosch, T. and Resnick, S. I. (2012). *Lévy processes: theory and applications*, Springer Science & Business Media.

Bjerksund, P. and Stensland, G. (2014). Closed form spread option valuation, *Quantitative Finance* **14**(10): 1785–1794.

Black, F. and Scholes, M. (1973). The pricing of options and corporate liabilities, *Journal of political economy* **81**(3): 637–654.

Bucklew, J. A. (2004). *Large Deviation Theory*, Springer New York, New York, NY, pp. 27–55.
https://doi.org/10.1007/978-1-4757-4078-3_3

Carmona, R. and Durrleman, V. (2003). Pricing and hedging spread options, *Siam Review* **45**(4): 627–685.

Carr, P. and Madan, D. (1999). Option valuation using the fast Fourier transform, *Journal of computational finance* **2**(4): 61–73.

Chung, K. L. (2001). *A course in probability theory*, Academic press.

Copeland, T. E. and Keenan, P. T. (1998). How much is flexibility worth?, *The McKinsey Quarterly* pp. 38–50.

Da Fonseca, J., Grasselli, M. and Tebaldi, C. (2007). Option pricing when correlations are stochastic: an analytical framework, *Review of Derivatives Research* **10**(2): 151–180.

Dempster, M. A. H. and Hong, S. G. (2002). Spread option valuation and the fast Fourier transform, *Mathematical Finance-Bachelier Congress 2000*, Springer, pp. 203–220.

Detemple, J., Feng, S. and Tian, W. (2003). The valuation of American call options on the minimum of two dividend-paying assets, *The Annals of Applied Probability* **13**(3): 953–983.

Dushimimana, J. C. (2010). *Pricing multi-asset options with Lévy copulas*, Master's thesis, Stellenbosch University.

Eberlein, E., Glau, K. and Papapantoleon, A. (2010). Analysis of Fourier transform valuation formulas and applications, *Applied Mathematical Finance* **17**(3): 211–240.

Fang, F. and Oosterlee, C. W. (2008). A novel pricing method for European options based on Fourier-cosine series expansions, *SIAM Journal on Scientific Computing* **31**(2): 826–848.

Figueroa-López, J. E., Lancette, S. R., Lee, K. and Mi, Y. (2011). Estimation of NIG and VG models for high frequency financial data.

Fiorani, F. (2004). Option pricing under the variance gamma process.

Gil-Pelaez, J. (1951). Note on the inversion theorem, *Biometrika* **38**(3-4): 481–482.

Godfrey, P. (2001). A note on the computation of the convergent Lanczos complex gamma approximation, *Web published at http://my. fit. edu/˜ gabdo/paulbio. html* .

Göncü, A., Karahan, M. O. and Kuzubas, T. U. (2013). Fitting the variance-gamma model: A goodness-of-fit check for emerging markets, *Bogazici Journal of Economics and Administrative Sciences* **27**(2): 1–10.

Guillaume, T. (2008). Making the best of best-of, *Review of Derivatives Research* **11**(1): 1–39.

Hurd, T. R. and Zhou, Z. (2010). A Fourier transform method for spread option pricing, *SIAM Journal on Financial Mathematics* **1**(1): 142–157.

Joshi, M. (2001). Log-type models, homogeneity of option prices and convexity, *QUARC, Royal Bank of Scotland working paper* .

Kienitz, J. and Wetterau, D. (2012). *Financial modelling: Theory, implementation and practice with matlab source*, John Wiley & Sons.

Kirk, E. (1995). Correlation in the energy markets, *Managing energy price risk* **1**: 71–78.

Klyueva, E. (2014). *Pricing and hedging tools for spread option contracts*, Master's thesis, University of Toronto.

Lanczos, C. (1964). A precision approximation of the gamma function, *Journal of the Society for Industrial and Applied Mathematics, Series B: Numerical Analysis* **1**(1): 86–96.

Leoni, P. and Schoutens, W. (2008). Multivariate smiling, *Wilmott Magazine* .

Madan, D. B., Carr, P. P. and Chang, E. C. (1998). The variance gamma process and option pricing, *European finance review* **2**(1): 79–105.

Madan, D. B. and Seneta, E. (1990). The variance gamma (VG) model for share market returns, *Journal of business* pp. 511–524.

Meng, Q.-J. and Ding, D. (2013). An efficient pricing method for rainbow options based on two-dimensional modified sine–sine series expansions, *International Journal of Computer Mathematics* **90**(5): 1096–1113.

Olivares, P. and Cane, M. (2014). Pricing spread options under stochastic correlation and jump-diffusion models, *arXiv preprint arXiv:1409.1175* .

Ouwehand, P. and West, G. (2006). Pricing rainbow options, *Wilmott magazine* **5**: 74–80.

Press, W. H., Flannery, B. P., Teukolsky, S. A. and Vetterling, W. T. (1989). Numerical recipes.

Ruijter, M. J. and Oosterlee, C. W. (2012). Two-dimensional Fourier cosine series expansion method for pricing financial options, *SIAM Journal on Scientific Computing* **34**(5): B642–B671.

Schoutens, W. (2003). *Lévy Processes in Finance*, Wiley: New York.

Stulz, R. (1982). Options on the minimum or the maximum of two risky assets: analysis and applications, *Journal of Financial Economics* **10**(2): 161–185.

Tankov, P. (2003). *Financial modelling with jump processes*, Vol. 2, CRC press.

Tankov, P. (2011). Pricing and hedging in exponential Lévy models: review of recent results, *Paris-Princeton Lectures on Mathematical Finance 2010*, Springer, pp. 319–359.

Touchette, H. (2009). The large deviation approach to statistical mechanics, *Physics Reports* **478**(1): 1–69.

Wang, J. (2009). *The multivariate variance gamma process and its applications in multi-asset option pricing*, PhD thesis.

Appendix A

Full Tables of Results

A.1 Spread

A.1.1 Black Scholes

Monte Carlo - 5 Million Simulations

Tab. A.1: Monte Carlo GBM spread option prices and standard deviations

Monte-Carlo Spread Prices and Standard Deviations								
Strike	**0.5**	**1**	**1.5**	**2**	**2.5**	**3**	**3.5**	**4**
Price	8.263795	8.016259	7.778114	7.544227	7.312432	7.091627	6.873904	6.653237
SD	0.005298	0.005229	0.005167	0.005103	0.005037	0.004976	0.004910	0.004840

Fast-Fourier Transform Method

Tab. A.2: GBM spread option prices using FFT

FFT-Method Price Estimates							
Strike	**BS**	**N = 32**	**N = 64**	**N =128**	**N = 256**	**N = 512**	**N = 1024**
90	8.262785	8.410911	8.245659	8.262590	8.262585	8.262651	8.262697
92	8.017495	8.216954	8.009094	8.017342	8.01734	8.017398	8.017398
94	7.777345	8.056394	7.774998	7.777176	7.777175	7.777242	7.777284
96	7.542322	7.818927	7.546463	7.542157	7.542156	7.542224	7.542266
98	7.312406	7.714239	7.325288	7.312292	7.312292	7.312341	7.312341
100	7.087575	7.487172	7.099942	7.087490	7.087489	7.087489	7.087528
102	6.867802	7.261733	6.892020	6.867735	6.867734	6.867734	6.867767
104	6.653058	7.039171	6.675566	6.653005	6.653005	6.653005	6.653031

For more clarity on the accuracy of the FFT estimates one can calculate the difference between the BS closed-form price and the estimate, as presented below:

Tab. A.3: Deviations between the BS price and the FFT-estimates

	FFT-Deviations From Closed-Form					
Strike	**N = 32**	**N = 64**	**N =128**	**N = 256**	**N = 512**	**N = 1024**
0.5	0.148126	-0.017130	-0.000195	-0.000200	-0.000133	-8.80E-05
1	0.199459	-0.008401	-0.000153	-0.000155	-0.000097	-9.69E-05
1.5	0.279048	-0.002348	-0.000170	-0.000171	-0.000104	-6.13E-05
2	0.276605	0.004141	-0.000165	-0.000165	-0.000098	-5.59E-05
2.5	0.401833	0.012882	-0.000113	-0.000114	-0.000065	-6.45E-05
3	0.399598	0.012368	-8.52E-05	-8.58E-05	-0.000086	-4.67E-05
3.5	0.393930	0.024218	-6.71E-05	-6.77E-05	-0.000068	-3.56E-05
4	0.386113	0.022509	-5.32E-05	-5.32E-05	-0.000053	-2.72E-05

Cosine-Method

Tab. A.4: GBM spread option prices using COS-method

	COS-Method Price Estimates						
Strike	**BS**	**N = 16**	**N = 32**	**N = 64**	**N = 128**	**N = 256**	**N = 512**
0.5	8.262785	8.202861	8.262457	8.262797	8.262797	8.262797	8.262797
1	8.017495	7.958374	8.017157	8.017496	8.017496	8.017496	8.017496
1.5	7.777345	7.718886	7.777008	7.777347	7.777347	7.777347	7.777347
2	7.542322	7.484375	7.541985	7.542324	7.542324	7.542324	7.542324
2.5	7.312406	7.254816	7.312070	7.312409	7.312409	7.312409	7.312409
3	7.087575	7.030180	7.087241	7.087579	7.087579	7.087579	7.087579
3.5	6.867802	6.810435	6.867469	6.867808	6.867808	6.867808	6.867808
4	6.653058	6.595548	6.652727	6.653065	6.653065	6.653065	6.653065

Again, one can express these prices using the difference between these estimates and the closed form prices:

Tab. A.5: Deviations between the BS price and the COS-estimates

	COS-Method Deviations From Closed-Form					
Strike	**N = 16**	**N = 32**	**N = 64**	**N = 128**	**N = 256**	**N = 512**
0.5	-0.059924	-0.000328	1.24E-05	1.24E-05	1.24E-05	1.24E-05
1	-0.059121	-0.000338	5.51E-07	5.56E-07	5.56E-07	5.56E-07
1.5	-0.058459	-0.000337	1.59E-06	1.59E-06	1.59E-06	1.59E-06
2	-0.057947	-0.000337	1.90E-06	1.91E-06	1.91E-06	1.91E-06
2.5	-0.057590	-0.000336	2.87E-06	2.88E-06	2.88E-06	2.88E-06
3	-0.057395	-0.000334	3.99E-06	4.00E-06	4.00E-06	4.00E-06
3.5	-0.057367	-0.000333	5.85E-06	5.85E-06	5.85E-06	5.85E-06
4	-0.057510	-0.000331	7.12E-06	7.13E-06	7.13E-06	7.13E-06

A.1.2 Variance-Gamma

Monte Carlo - 5 Million Simulations

Tab. A.6: Monte Carlo VG spread option prices and standard deviations

Monte-Carlo Spread Option Prices ad Standard Deviations								
	0.5	**1**	**1.5**	**2**	**2.5**	**3**	**3.5**	**4**
Price	8.203884	7.924505	7.649759	7.379730	7.114484	6.854099	6.598628	6.348127
SD	0.004580	0.004505	0.004430	0.004353	0.004277	0.004199	0.004122	0.004043

Fast Fourier Transform

Tab. A.7: VG spread option prices using FFT-method

FFT-Method Estimates						
Strike	**N = 32**	**N = 64**	**N =128**	**N = 256**	**N = 512**	**N = 1024**
0.5	8.629405	8.315092	8.213579	8.213042	8.212581	8.213680
1	8.399087	8.040854	7.933597	7.933023	7.933030	7.933639
1.5	8.201387	7.763785	7.658840	7.658133	7.658865	7.658866
2	7.918389	7.499512	7.388622	7.387840	7.387307	7.388638
2.5	7.779384	7.247325	7.122638	7.121974	7.121976	7.122649
3	7.509724	6.969022	6.861733	6.861739	6.861132	6.861741
3.5	7.241009	6.735073	6.605873	6.605877	6.605291	6.605878
4	6.974860	6.468787	6.355078	6.354476	6.354477	6.355081

Cosine Method

Tab. A.8: VG spread option prices using COS-method

Cos-Method Price Estimates						
Strike	**N = 32**	**N = 64**	**N =128**	**N = 256**	**N = 512**	**N = 1024**
0.5	-13.82103	8.875529	8.223157	8.211935	8.212066	8.212066
1	-14.09826	8.593991	7.943111	7.931893	7.932025	7.932025
1.5	-14.37124	8.317667	7.668517	7.657301	7.657433	7.657433
2	-14.64045	8.045613	7.398191	7.386966	7.387099	7.387099
2.5	-14.90565	7.778395	7.132903	7.121681	7.121814	7.121814
3	-15.16687	7.515871	6.872321	6.861071	6.861204	6.861204
3.5	-15.42408	7.258148	6.616714	6.605461	6.605595	6.605595
4	-15.67722	7.005316	6.366068	6.354774	6.354908	6.354908

A.2 Worst Of Rainbow Options

A.2.1 Black Scholes

Monte Carlo - 5 Million Simulations

Tab. A.9: Monte Carlo GBM rainbow option prices and standard deviations

Monte-Carlo Spread Option Prices ad Standard Deviations								
	90	**92**	**94**	**96**	**98**	**100**	**102**	**104**
Price	8.269110	7.120108	6.056911	5.088743	4.220256	3.457143	2.786758	2.213518
SD	0.004059	0.003806	0.003540	0.003265	0.002985	0.002707	0.002429	0.002159

Fast-Fourier Transform Method

Tab. A.10: GBM rainbow options using FFT-method

FFT-Method Price Estimates								
Strike	**Stulz**	**N = 32**	**N = 64**	**N = 128**	**N = 256**	**N = 512**	**N = 1024**	**N = 2048**
ū		**10**	**30**	**50**	**90**	**120**	**130**	**130**
90	8.274176	10.30290	8.503732	8.279946	8.277714	8.276344	8.276344	8.276344
92	7.118883	11.40277	7.979664	7.171976	7.122597	7.118973	7.118973	7.118973
94	6.055238	17.90643	9.801668	6.827704	6.059106	6.055460	6.055238	6.055238
96	5.087925	5.088197	5.049985	5.091439	5.087805	5.087909	5.088155	5.088155
98	4.220092	4.220273	4.194226	4.214949	4.221059	4.220421	4.220358	4.220358
100	3.452949	3.452872	3.463136	3.453683	3.454077	3.452917	3.452865	3.452865
102	2.785485	2.785165	2.822560	2.793159	2.785546	2.785078	2.785089	2.785089
104	2.214392	2.214116	2.246806	2.214755	2.216092	2.214516	2.214276	2.214276

Tab. A.11: Deviations between the Stulz price and the FFT-estimates

Deviations between the Stulz price and the FFT-estimates							
Strike	**N = 32**	**N = 64**	**N =128**	**N = 256**	**N = 512**	**N = 1024**	**N =2048**
90	2.028720	0.229556	0.005770	0.003538	0.002168	0.002168	0.002168
92	4.283891	0.860780	0.053093	0.003714	8.98E-05	8.98E-05	8.98E-05
94	11.85119	3.746430	0.772465	0.003868	0.000222	-4.07E-08	-4.53E-08
96	0.000272	-0.037939	0.003515	-0.000120	-1.60E-05	0.000231	0.000231
98	0.000181	-0.025865	-0.005143	0.000967	0.000329	0.000266	0.000266
100	-0.000076	0.010187	0.000734	0.001128	-3.19E-05	-8.35E-05	-8.35E-05
102	-0.000320	0.037075	0.007674	0.000060	-0.000407	-0.000397	-0.000397
104	-0.000276	0.032414	0.000363	0.001699	0.000124	-0.000116	-0.000116

Cosine-Method

Tab. A.12: GBM rainbow option prices using COS-method

COS-Method Price Estimates								
Strike	**Stulz**	**N=16**	**N = 32**	**N = 64**	**N =128**	**N = 256**	**N = 512**	**N = 1024**
90	8.274176	8.051463	8.275085	8.274245	8.274245	8.274245	8.274245	8.274245
92	7.118883	6.930400	7.116345	7.118949	7.118949	7.118949	7.118949	7.118949
94	6.055238	5.913286	6.049725	6.055240	6.055239	6.055239	6.055239	6.055239
96	5.087925	5.000499	5.080858	5.088021	5.088002	5.088020	5.088020	5.088020
98	4.220092	4.189836	4.212929	4.220139	4.220139	4.220139	4.220139	4.220139
100	3.452949	3.477785	3.447202	3.452955	3.452955	3.452955	3.452955	3.452955
102	2.785485	2.859236	2.782285	2.785522	2.785523	2.785523	2.785523	2.785523
104	2.214392	2.327786	2.214169	2.214472	2.214472	2.214472	2.214472	2.214472

Again, for clarity, we can look at the differences between the COS-estimates and the Stulz closed-form approximation

Tab. A.13: Deviations between the Stulz price and the COS-estimates

COS-Method Deviations from Stulz Price							
Strike	**N = 16**	**N = 32**	**N = 64**	**N = 128**	**N = 256**	**N = 512**	**N = 1024**
90	-0.222713	0.000909	6.93E-05	6.94E-05	6.94E-05	6.94E-05	6.94E-05
92	-0.188483	-0.002538	6.59E-05	6.56E-05	6.56E-05	6.56E-05	6.56E-05
94	-0.141953	-0.005514	1.50E-06	9.56E-07	9.56E-07	9.56E-07	9.56E-07
96	-0.087425	-0.007066	9.63E-05	9.59E-05	9.59E-05	9.59E-05	9.59E-05
98	-0.030256	-0.007163	4.75E-05	4.75E-05	4.75E-05	4.75E-05	4.75E-05
100	0.024837	-0.005747	6.01E-06	6.40E-06	6.40E-06	7.98E-05	7.98E-05
102	0.073750	-0.003200	3.66E-05	3.71E-05	3.71E-05	3.71E-05	3.71E-05
104	0.113393	-0.000223	7.95E-05	7.98E-05	7.98E-05	7.98E-05	7.98E-05

A.2.2 Variance-Gamma

Monte Carlo – 5 Million Simulations

Tab. A.14: Monte Carlo GBM rainbow option prices and standard deviations

Monte-Carlo Spread Option Prices ad Standard Deviations								
	90	**92**	**94**	**96**	**98**	**100**	**102**	**104**
Price	15.70534	14.70500	13.74129	12.81444	11.92467	11.07196	10.256400	9.477602
SD	0.009688	0.009373	0.009054	0.008732	0.008408	0.008082	0.007755	0.007428

Fast-Fourier Transform Method

Tab. A.15: VG rainbow option prices using FFT-method

	FFT-Method Price Estimates							
Strike	**N = 32**	**N = 64**	**N =128**	**N = 256**	**N = 512**	**N = 1024**	**N =2048**	**N = 4096**
ū	**20**	**30**	**50**	**80**	**130**	**140**	**170**	**170**
90	15.70112	15.71367	15.71456	15.70917	15.70820	15.70845	15.70839	15.70839
92	14.65523	14.71581	14.70609	14.70774	14.70785	14.70804	14.70788	14.70788
94	13.68651	13.73797	13.74777	13.74433	13.74425	13.74433	13.74408	13.74408
96	12.78901	12.80185	12.82235	12.81765	12.81754	12.81750	12.81722	12.81722
98	11.93510	11.90962	11.92409	11.92720	11.92771	11.92760	11.92740	11.92740
100	11.11774	11.07365	11.07668	11.07525	11.07466	11.07463	11.07465	11.07465
102	10.30499	10.26620	10.26399	10.25840	10.25855	10.25862	10.25890	10.25890
104	9.488523	9.475121	9.476305	9.480437	9.479729	9.479659	9.480024	9.480024

Cosine-Method

Tab. A.16: VG rainbow option prices using COS-method

	COS-Method Prices						
Strike	**N = 16**	**N = 32**	**N = 64**	**N = 128**	**N = 256**	**N = 512**	**N = 1024**
90	26.09983	16.20615	15.73860	15.70947	15.70934	15.70934	15.70934
92	25.34483	15.22061	14.73720	14.70899	14.70889	14.70889	14.70889
94	24.62656	14.27847	13.77228	13.74523	13.74514	13.74514	13.74514
96	23.94375	13.37988	12.84400	12.81840	12.81829	12.81829	12.81829
98	23.29508	12.52471	11.95249	11.92859	11.92844	11.92843	11.92843
100	22.67918	11.71262	11.09778	11.07575	11.07554	11.07554	11.07554
102	22.09466	10.94304	10.27983	10.25971	10.25945	10.25945	10.25945
104	21.54064	10.21589	9.499151	9.480784	9.480513	9.480512	9.480512

Appendix B

The Hurd and Zhou (2010) Method on Worst of Options

B.1 Truncation Errors

The requirement of a choice of value for $\bar{u}$ along with the maintenance of the Nyquist relationship leads to the need to evaluate the truncation error for various values of $\bar{u}$ and N across all strike prices. Below the truncation error associated with pricing under GBM is illustrated for a strike price of 98; in general the higher the value of $\bar{u}$ the greater the error for lower N and the smaller the error for high N as illustrated below.

Fig. B.1: Comparison of all choices of $\bar{u}$

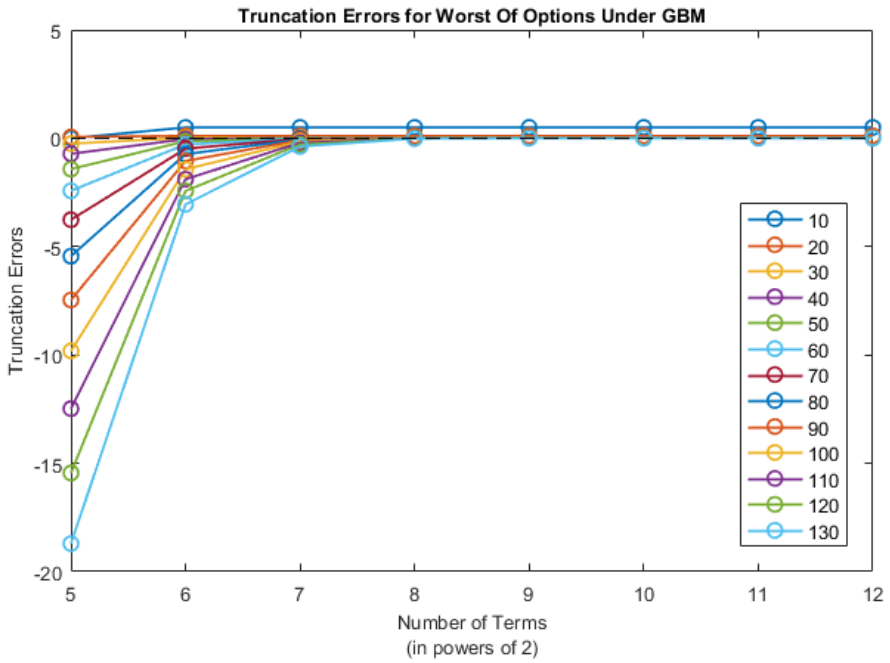

Thus, one would need to use different values of $\bar{u}$ for different N. Taking a deeper look and dividing up the $\bar{u}$ values into smaller subgroups, one can see the relative errors across N.

Fig. B.2: Comparison of groups of $\bar{u}$

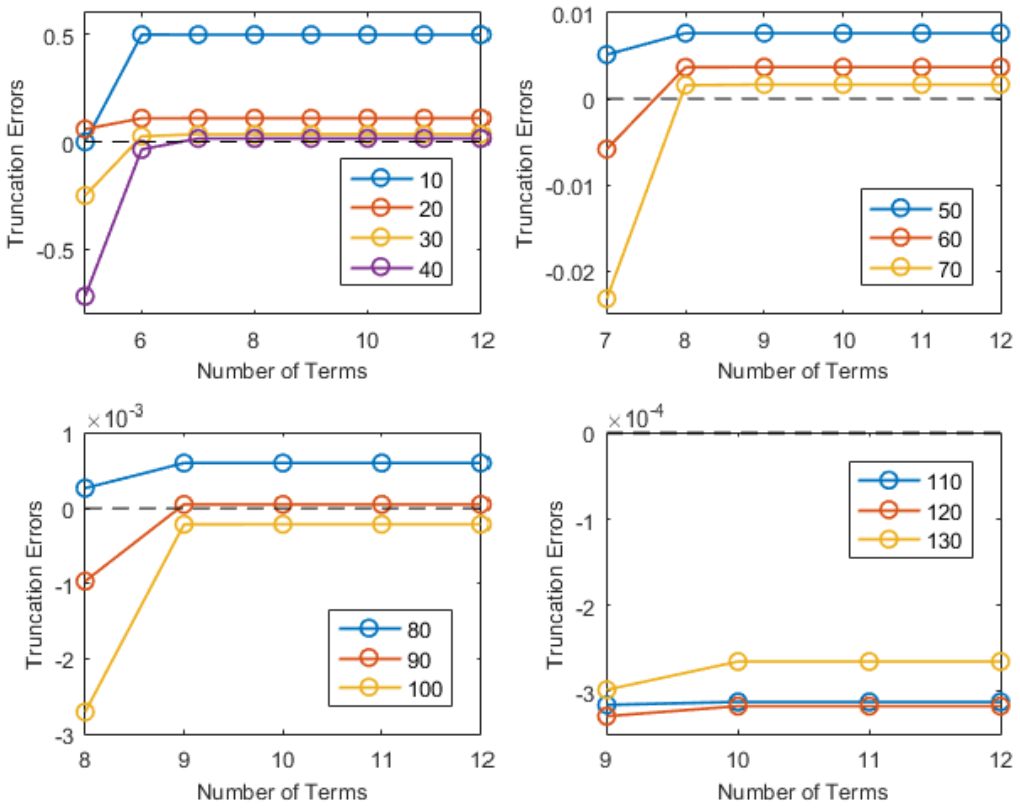

Values from 10 to 130 with increments of 10 were considered, and the value that minimised the sum of the absolute errors across all strike prices was chosen for that value of N. It is worth noting that the truncation errors for each $\bar{u}$ and N varied only very slightly across strike prices.